RSC Advances

REVIEW

View Article Online
View Journal | View Issue

Cite this: *RSC Adv.*, 2024, **14**, 14722

Manganese-based nanomaterials in diagnostics and chemodynamic therapy of cancers: new development

Meiyan Wu, †[a] Yuan Liao, †[a] Di Guo,[a] Mingyue Zhai,[a] Desong Xia,[a] Zhikun Zhang,*[b] Xiyu Liu*[a] and Yong Huang*[a]

In the realm of cancer treatment, traditional modalities like radiotherapy and chemotherapy have achieved certain advancements but continue to grapple with challenges including harm to healthy tissues, resistance to treatment, and adverse drug reactions. The swift progress in nanotechnology recently has opened avenues for investigating innovative approaches to cancer therapy. Especially, chemodynamic therapy (CDT) utilizing metal nanomaterials stands out as an effective cancer treatment choice owing to its minimal side effects and independence from external energy sources. Transition metals like manganese are capable of exerting anti-tumor effects through a Fenton-like mechanism, with their distinctive magnetic properties playing a crucial role as contrast agents in tumor diagnosis and treatment. Against this backdrop, this review emphasizes the recent five-year advancements in the application of manganese (Mn) metal ions within nanomaterials, particularly highlighting their unique capabilities in catalyzing CDT and enhancing MRI imaging. Initially, we delineate the biomedical properties of manganese, followed by an integrated discussion on the utilization of manganese-based nanomaterials in CDT alongside multimodal therapies, and delve into the application and future outlook of manganese-based nanomaterial-mediated MRI imaging techniques in cancer therapy. By this means, the objective is to furnish novel viewpoints and possibilities for the research and development in future cancer therapies.

Received 3rd March 2024
Accepted 17th April 2024

DOI: 10.1039/d4ra01655f

rsc.li/rsc-advances

1 Introduction

As indicated by recent cancer statistics,[1] cancer remains a significant challenge to human well-being, with the advancement of effective therapies being a primary aim of cancer nanomedicine.[2] Presently, radiotherapy and chemotherapy still form the foundation of clinical cancer treatments.[3] While significant achievements have been made with these two treatments, ionizing radiation can irreversibly harm adjacent normal tissues, thus restricting the radiation dose delivered to the patient.[4] Additionally, resistance and toxicity associated with chemotherapy can lead to various side effects in patients,[5] indicating certain limitations in these therapies. The burgeoning growth of biotechnology and nanotechnology in recent years has revitalized new therapeutic approaches. In 2016, Tang and his team initially coined the term CDT.[6] Due to its reduced side effects and the absence of a need for external energy sources, it has emerged as an effective method for treating cancer.[7] CDT is driven by the Fenton reaction and Fenton-like reaction,[8] which are considered potential strategies for tumor cell treatment.[9] The Fenton reaction involves Fe^{2+}/Fe^{3+} redox, catalyzing intracellular hydrogen peroxide (H_2O_2) to produce highly toxic ROS. Fenton-like processes encompass reactions in which Fe^{3+}, iron-bearing minerals, and various transition metals, including Cu, Ag, Mn, and Ni, can expedite or act as surrogates for Fe^{2+} in the catalysis of H_2O_2.[10] For radiotherapy and chemotherapy, high doses of drugs can cause severe damage to normal tissues, and even peripheral neuropathy in cases of overexpression and permanent sequelae and disability in a large percentage of cancer survivors.[11,12] In addition, compared with photodynamic therapy (PDT), CDT does not produce complications such as pain, burns, and oedema.[12] At the same time, CDT does not require exogenous stimulation and there is no damage to normal tissues caused by the high-frequency ultrasound in sonodynamic therapy (SDT). Therefore, CDT is currently widely regarded as a new treatment method with fewer side effects.[13]

Owing to the presence of various electrolyte ions (like calcium and phosphates) and bioactive groups in tissues and cells, they could influence CDT through chelation with iron ions or reaction with cytotoxic hydroxyl radicals (˙OH).[14] Many research findings show that the efficacy of CDT in treating

[a]*State Key Laboratory of Targeting Oncology, National Center for International Research of Bio-Targeting Theranostics, Guangxi Key Laboratory of Bio-Targeting Theranostics, Collaborative Innovation Center for Targeting Tumor Diagnosis and Therapy, Guangxi Medical University, Nanning 530021, China. E-mail: huangyong503@126.com; liuxiyu0509@sr.gxmu.edu.cn*

[b]*The Second Affiliated Hospital of Guangxi Medical University, China. E-mail: zzkicecream@163.com*

† These authors contributed equally to this work.

cancer is frequently constrained by the proportion of metal ions, requiring the addition of low-valent metal ions in the synthesis of nanomaterials to boost CDT's effectiveness.[15] Nanomaterials with Mn^{2+} may boost CDT by triggering oxidative stress responses in cells due to the released Mn^{2+}, and also act as MRI contrast agents for tumor imaging during the therapeutic process.[16] Modern medical imaging modalities, including X-ray computed tomography (CT), positron emission tomography (PET), and magnetic resonance imaging (MRI), play a pivotal role in therapeutic interventions. MRI stands out from CT and PET scans as it does not expose the body to radiation, and is extensively used in clinics for medical diagnosis, disease staging, and follow-ups. Laboratory research benefits from the visualization of tumor sites, contributing to the early detection of tumors. Integrating therapy with diagnosis to enable concurrent therapy monitoring and diagnosis is an anticipated and ideal direction in the recent advancements of functional imaging technology.

Therefore, this review first introduces the biomedical properties of manganese, and starting from its CDT and MRI characteristics, it focuses on the diverse applications of manganese (Mn)-based nanomaterials in CDT, and delves into the application prospects of its longitudinal relaxation time (T_1)-enhanced MRI characteristics combined with various imaging methods in precise tumor monitoring and treatment, aiming to suggest ways to enhance the application depth and breadth of manganese-based nanomaterials in the future.

2 Manganese's biological characteristics

Manganese, found in minuscule quantities in the cells of living organisms, is a vital trace element necessary for the life processes of both animals and plants. It performs numerous physiological roles, encompassing not just the promotion of bone growth and development, and the maintenance of normal glucose and fat metabolism, but also exerting a significant influence on oxidative stress and hematopoiesis. Significantly, Mn exhibits distinct functionalities in nanomedicine, such as immune defense, CDT, MRI, and TME reconstruction, offering ample prospects for the development of versatile nanomedicine platforms. The specific attributes of Mn are outlined below (Fig. 1), anticipated to inform the design of Mn-based multifunctional nano-platforms.

2.1 Physiological functions

Manganese, both a necessary nutrient and a crucial heavy metal, is found naturally in the environment. The daily required energy for functions such as antioxidation, energy metabolism, immune function, and others are obtained through dietary sources.[17] It forms part of several physiologically important enzymes and is a necessary cofactor for various enzyme systems, including manganese-specific glycosyltransferases and phosphoenolpyruvate carboxylase. Such enzymes are instrumental in regulating metabolic activities including cholesterol synthesis, gluconeogenesis, and cartilage development.[18] The United States Food and Drug Administration (FDA) suggests the daily intake of manganese for adult males is 2.3 mg per day and for females 1.8 mg per day.[19] Leveraging its catalytic and redox capabilities, manganese modulates a spectrum of enzymes, including manganese superoxide dismutase (SOD), glutamine synthetase, and pyruvate carboxylase, among others. This modulation plays a crucial role in maintaining the metabolic balance and redox equilibrium vital to life's processes. Furthermore, manganese superoxide dismutase (MnSOD) serves as the principal antioxidant within mitochondria, capable of catalyzing the decomposition of superoxide radicals into hydrogen peroxide to achieve a tumor-killing effect.[20] *Via* these metalloenzymes, manganese is instrumental in numerous biological processes including development, digestion, reproduction, antioxidative protection, energy generation, immune response, and the control of neuronal activity.[21] Manganese has been shown to enhance the immune responses in vertebrates, including humans, rodents, birds, and fish.[22] Conversely, excess manganese tends to accumulate in the liver, pancreas, bones, kidneys, and brain, with the brain being the main target for manganese toxicity, causing neurotoxicity and other detrimental impacts.[21] The imbalance of manganese in neurological conditions highlights its critical role in brain development and essential neurophysiological functions. Genetic disorders affecting manganese transport, resulting in neurodevelopmental and neurodegenerative syndromes, underscore its neurotoxic capacity. Additionally, disruptions in manganese balance are associated with Parkinson's disease and other neurodegenerative diseases, including Alzheimer's disease and Huntington's disease.[23] Within the human brain, typical Mn concentrations range from 20.0 μM to 52.8 μM, and when Mn concentrations are between 60.1 and 158.4 μM, brain function becomes abnormal.[24] The normal range for free manganese concentration in the blood is between 0.029 and 1.2 μM, and it is within this range that the application of Mn-based nanomaterials is deemed safe.[25]

2.2 Chemodynamic therapy and tumor microenvironment regulation

Chemodynamic therapy (CDT) represents a novel therapeutic approach, which involves *in situ* treatment at the tumor site by generating $^{\bullet}OH$ through Fenton or Fenton-like reactions. Manganese, among other metal nanomaterials, has Fenton or Fenton-like properties that dissolve into metal ions under the mildly acidic conditions of the TME, initiating the Fenton reaction to produce excess H_2O_2, generating $^{\bullet}OH$, thereby triggering cell apoptosis and inhibiting tumors.[6,26] The tumor microenvironment (TME) is distinguished by mild acidity, elevated H_2O_2 concentrations, reduced catalase activity, and hypoxia, providing an optimal environment and nutrients that facilitate tumor growth and metastasis, making it an ideal target for tumor therapy.[6,27] Tumor cells are chiefly characterized by elevated Reactive Oxygen Species (ROS) levels and changes in redox state. ROS denotes substances with high oxidative potential featuring oxygen radicals, encompassing peroxides, superoxides, singlet oxygen, and hydroxyl radicals

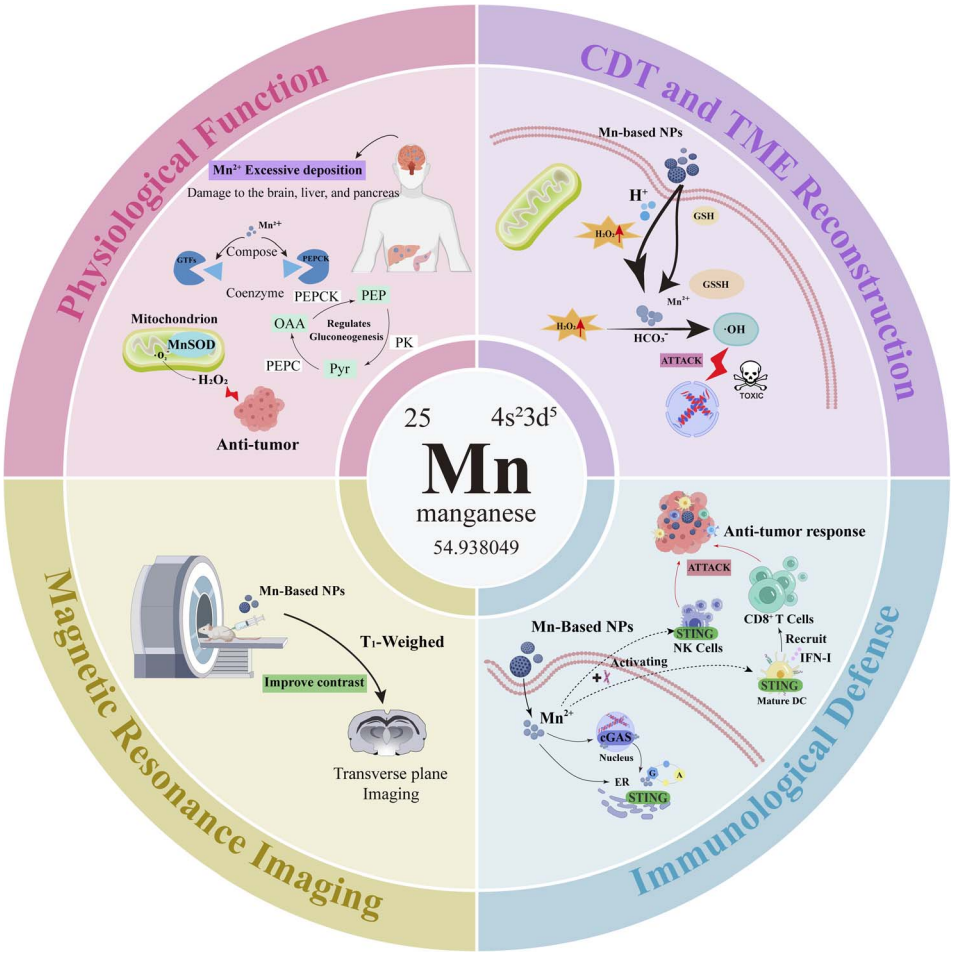

Fig. 1 Manganese has the following four main functions: (1) physiological functions; (2) chemodynamic therapy and tumor microenvironment regulation; (3) immune defense; (4) magnetic resonance imaging.

among others.[26,28,29] Within organisms, ROS serve as crucial cellular signaling molecules, playing a key role in the regulation of diverse physiological processes and the maintenance of the cells' normal redox equilibrium. The generation of endogenous ROS primarily originates from the aerobic metabolism in cellular mitochondria. Under normal physiological conditions, the concentration of ROS can be regulated to remain within a stable range, playing a significant role in regulating cell signaling, bacterial clearance, mediating inflammation, and adjusting protein functions among other metabolic pathways.[30] When ROS levels surpass the tolerance threshold, it can result in oxidative stress, leading to irreversible, nonspecific damage to proteins, lipids, and DNA. The delivery characteristics of Mn^{2+} and the consumption behavior of glutathione help to tackle the issue of diminished CDT effectiveness due to the reduction of intracellular glutathione (GSH).[31] The increase in cytotoxic hydroxyl radicals (˙OH) can induce DNA and protein damage, accelerating the apoptosis of cancer cells. It has also been found that MnO_2 nanostructures decompose H_2O_2 in the TME, achieving an effect of alleviating tumor hypoxia.[32] The process involves MnO_2 nanoparticles undergoing redox reactions, producing Mn^{2+} and glutathione disulfide (GSSG), consuming the overexpressed antioxidant GSH in cells, significantly reducing its content, and increasing the sensitivity of tumor cells to ROS. Furthermore, within the acidic conditions of the tumor microenvironment (TME), MnO_2 nanoparticles interact with the excessively present H_2O_2 in the tumor, generating a significant quantity of oxygen.[33] In addition to Mn-based nanomaterials, other nanomaterials capable of inducing CDT include other metal nanomaterials (such as iron-based, copper-based, *etc.*), silicon-based nanomaterials, and carbon-based nanomaterials, all of which have certain defects in their application. The Fenton reaction is primarily catalyzed by low-valence metal ions, but the low reaction rate of the reduction of Fe^{3+} to Fe^{2+} greatly limits the Fenton reaction.[34] Moreover, Cu exhibits greater toxicity than Fe or Mn in usage.[35] Silicon-based nanomaterials are often used as auxiliary nanomaterials, making it difficult to promote the Fenton reaction process and resulting in extremely slow degradation speeds. Furthermore, the high-temperature carbonization process used in the preparation of carbon-based nanomaterials does not allow for the uniform dispersion of the target carriers, leading to the risk of highly aggregated nanomaterials in blood transport.[36] In contrast, Mn-based nanomaterials offer relatively safe and

efficient treatment, and advantageous for ROS/oxygen-dependent tumor therapy by modulating TME, which have great potential in tumor chemodynamic therapy.

2.3 Immune defense function

Mn plays an immunomodulatory role in the body.[37] Beyond altering the tumor microenvironment (TME), this approach also amplifies tumor treatment efficacy through the activation of Mn^{2+}-associated immune pathways, effectively responding to the TME conditions, thereby alleviating hypoxia, GSH depletion, and other immunosuppressive conditions. The stimulator of interferon genes (STING) promotes signal transduction and the production of type I IFN through the activation of the TBK1-IRF3 axis, and can directly participate in the detection of intracellular bacteria.[38] Cyclic GMP-AMP synthase (cGAS) produces the endogenous second messenger 2′3′-cyclic GMP-AMP (2′3′-cGAMP), which directly binds to STING, promoting its activation.[39] The early immune system's targeting and killing of tumor cells depend on dendritic cells (DCs) producing type I interferons (IFNs) and recruiting $CD8^+$ T cells, while the STING pathway plays a unique role in this critical step of anti-tumor immunity by attracting $CD8^+$ T cells to the TME.[40] Moreover, the cGAS-STING pathway can initiate the synthesis of antiviral cytokines belonging to the type I interferon family, leading to the induction of hundreds of interferon-stimulated genes (ISGs) that possess diverse antiviral activities.[41] Mn^{2+} act as potent activators of cGAS, triggering cells to produce type I IFNs and cytokines even without any infection. This activation markedly fosters the maturation and antigen presentation of DCs and macrophages in a cGAS-STING-dependent way, enhancing the activation of $CD8^+$ T cells and NK cells.[25] Additionally, Mn^{2+} boosts the detection of viral infections in cells by heightening the sensitivity of the DNA sensor cGAS and its downstream adaptor protein STING. It also promotes the activity of the STING pathway by strengthening the binding affinity of cGAMP-STING.[42] Based on these findings, Mn^{2+} demonstrates great potential in tumor immunology, with its product IFN-I having immunomodulatory functions, initiating anti-tumor responses through $CD8^+$ T and NK cells.

2.4 Magnetic resonance imaging

Magnetic Resonance Imaging (MRI), a medical imaging modality devoid of X-rays and ionizing radiation, has emerged as a crucial non-invasive technique for molecular imaging. This prominence is attributed to its unparalleled signal-to-noise ratio, superior spatial resolution, and exceptional contrast in soft tissues. Compared to CT scans, MRI is still considered a better choice. Commonly, paramagnetic metals as well as superparamagnetic and ferromagnetic substances are used as CAs due to their ability to magnetize in an external magnetic field.[43] Currently, the most frequently utilized T_1 paramagnetic metal contrast agents comprise Mn-based, gadolinium-based, and iron oxide-based agents,[44] while gadolinium-based contrast agents are clinically useful, they are associated with significant nephrotoxicity.[45] Furthermore, their short circulation time prevents the acquisition of high-resolution images, making them unsuitable for prolonged tissue scanning. The signal voids appearing in iron oxide-based contrast agents are indistinguishable from those produced by the metallic materials themselves, thus limiting their clinical application.[46] Mn-based contrast agents are effective MRI relaxants and are among the most common pH-responsive magnetic resonance nano-contrast agents. They are sensitive to the weakly acidic and reductive conditions of the TME. In an acidic environment, Mn(II) ions with five unpaired electrons can be released, increasing the likelihood of Mn(II) paramagnetic centers contacting water molecules, thus significantly shortening the longitudinal relaxation time of water protons, yielding robust high signals without adverse effects. Mn(II) can selectively enter neurons *via* voltage-gated calcium channels, inducing neuronal activity.[47] Within safe dosage limits, longitudinal imaging of the whole brain dynamics of the same subject can be repeated over several weeks.[48] Manganese contrast agents have similar positive contrast enhancement capabilities; binding with proteins can increase the relaxivity of Mn^{2+} and enhance contrast.[49] In relation to boosting the contrast in T_1 imaging for heightened sensitivity in cancer diagnosis, Yang *et al.*, focusing on nano-manganese oxide, discovered that the surface area, volume, and the r_2/r_1 ratio of manganese ions have both positive and negative impacts on the sensitivity of T_1 imaging. MnO octahedra, featuring a high longitudinal relaxation rate (r_1) value of 20.07 mM^{-1} s^{-1}, showed significant improvement in liver T_1 imaging. Furthermore, both liver and subcutaneous tumors remained detectable even at ultra-low dosages.[50] Based on these characteristics, manganese-based nanomaterials are CAs with broad application prospects in T_1-weighted MRI.

In summary, leveraging the ROS generation capabilities and other properties inherent to Mn^{2+} Fenton-like reactions, Mn^{2+} can be utilized across a spectrum of cancer treatment modalities, including CDT and immunotherapy. Its ability to modulate the TME amplifies the efficacy of cancer therapies. Additionally, its utility in MRI provides a means to track the progress of tumor treatment, ascertain the *in vivo* biological distribution, and assess the effectiveness of cancer therapies. Therefore, Mn-based nanomaterials offer the flexibility to be precisely engineered and developed into traceable, multifunctional nano-platforms for efficacious tumor therapy. Here, we provide a brief introduction to the research progress on the application of manganese-based multifunctional nano-platforms in CDT therapy, including multimodal synergistic treatments related to CDT and imaging-guided tumor therapy. Finally, we explore the obstacles and prospective advancements in the application of Mn-based CDT for cancer treatment.

3 Chemodynamic therapy involving multimodal synergistic treatment

Normally, natural CDT agents (such as Fe ions) are present in the body, but the low concentration of Fe ions in cancer cells results in reduced Fenton reaction efficiency, rendering the amount of catalytically generated ˙OH insufficient to trigger apoptosis in cancer cells. Conversely, Mn-based nanomaterials

can supply ample CDT agents, facilitating CDT therapy, and when used in conjunction with other therapies, they can further enhance the efficacy of tumor treatment. Meanwhile, Mn-based nanomaterials, as nanomedicines, satisfy the properties of stability, biodegradability, biocompatibility and targeting, and the advantage of targeting is also a major feature for CDT treatment. The following briefly introduces some Mn-based nanomaterials targeting CDT and summarises the pros and cons of certain therapies (including chemotherapy, radiotherapy, starvation therapy, gas therapy, PDT, PTT, and others), as well as studies on their combined treatment with CDT.

3.1 Mn-based nanomaterials targeting CDT

The commonly used cancer treatment modalities, such as surgery, radiation therapy, and chemotherapy, suffer from limitations like poor targeting, reduced effectiveness, and prolonged duration of action.[51] The significant rationale behind selecting nanomedicine for cancer therapy lies in the targeted approach of nanomedicines. Targeted nanoparticles are capable of directing drug delivery to the TME, managing the release schedule of the medication, minimizing the off-target adverse reactions and potential toxicity, which, in turn, improves the outcomes of cancer therapy.[52] A common method to improve the targeting of nanomaterials is to modify the surface of nanoparticles with different small molecules to increase specific binding affinity, thereby achieving targeting of specific sites or cells.[53] Chen *et al.* designed nanohybrids (TSMs), which use transferrin (Tf) as a modified small molecule to target the overexpression of the transferrin receptor (TfR) on the surface of cancer cells, and can deliver the nanomedicine targeted delivery to subcutaneous tumor sites. Meanwhile, the other two components included in TSM, MnO_2 and semiconductor polymers (SP), also play different anti-tumor roles; manganese dioxide can be used as a catalyst for CDT, and semiconductor polymers can be used as a nanophotosensitizer for PDT, mediating the combined treatment of PDT and CDT and generating abundant ROS, thus enhancing the targeted anti-tumor effect.[54] Besides Tf, there are many commonly used small molecule ligands, including arginine-glycine-aspartate (RGD) peptide, triphenylphosphine (TPP), *etc.* For example, Li *et al.* modified RGD peptide on indocyanine green (ICG) labeled Mn-based nanomaterials carrying lncRNA OUM1 and its target gene siPTPRZ1 and cisplatin. Due to the specific binding of RGD peptide with the overexpressed integrin αvβ3 receptor on the tumor cell membrane, specific targeting of tumor cells can be achieved.[55] Zhong *et al.* designed a nanopreparation, TPP-DOX@MnBSA (TD@MB), which modifies DOX with TPP as a ligand, with mitochondria as the entry therapeutic target. TPP as a mitochondrial ligand can be absorbed by the mitochondrial membrane, and targeting TPP-DOX to the mitochondria can achieve tumor cell killing by destroying the mitochondria, while synergizing with Mn^{2+}-mediated CDT can amplify the tumor-killing effect.[56]

3.2 Mn-based CDT and chemotherapy

Chemotherapy stands as a prevalent anti-cancer drug modality for systemic therapy and ranks among the most potent methods for treating cancer. It primarily utilizes potent cytotoxic drugs that target rapidly dividing cells through various mechanisms to suppress tumor growth and prevent distant metastasis.[57] However, the use of these chemotherapy drugs is limited by resistance, selectivity, and inevitable side effects. They are only employed when their therapeutic benefits surpass their chemical toxicity, significantly constraining their effectiveness in treating malignancies and thus limiting their efficacy in cancer therapy.[57,58] Hence, pursuing treatments that target specific tumor sites in conjunction with other materials is a crucial developmental direction. Encapsulation or incorporation of drugs into nanocarriers can significantly enhance their solubility, stability, and bioavailability, thereby enabling targeted distribution within the body. Such modifications in the drugs' inherent physicochemical properties and delivery efficiency culminate in improved therapeutic outcomes for the encapsulated or loaded drugs.[59] Tumor tissues exhibit heterogeneity,[60] with a substantial presence of cells resistant to chemotherapy. Once most of the sensitive cells are eliminated, the remaining ones may develop resistance, potentially causing tumor resistance or recurrence. Zhong *et al.* developed TPP-DOX@MnBSA (TD@MB) nanoparticles, using bovine serum albumin (BSA) as a carrier, loaded with triphenylphosphine-modified doxorubicin (TPP-DOX) and manganese, to combine chemotherapy with CDT. The uniform and stable spherical nanoparticles enhance drug absorption and ensure mitochondrial targeted delivery, increasing intracellular ROS and highly toxic ˙OH, thereby effectively inhibiting the proliferation of both chemosensitive and chemoresistant MCF-7 breast cancer cells. Furthermore, TD@MB is capable of downregulating proteins associated with stem cells and metastasis, thereby decreasing the stemness and metastatic potential of tumors. *In vivo* experiments using a tumor-bearing zebrafish model demonstrated that TD@MB exhibits excellent anti-tumor effects, along with good tumor targeting and biocompatibility. *In vivo* experiments using the 4T1 tumor-bearing nude mouse model and the MCF-7 tumor-bearing zebrafish model were conducted to verify the biodistribution, excellent tumor targeting, and biocompatibility of TD@MB.[56]

3.3 Mn-based CDT and radiotherapy

Radiotherapy (RT) is a significant approach extensively utilized for cancer treatment in clinical settings. Its underlying mechanism entails the generation of ROS and other free radicals, leading to molecular structural damage, including DNA single and double-strand breaks. This process directly harms DNA, curtails cell proliferation, and may induce cell death or apoptosis.[61,62] However, the efficacy of radiotherapy is influenced by various factors. Initially, the tumor microenvironment's weak acidity, hypoxia, and high glutathione levels affect radiotherapy's outcomes.[63] Secondly, although hypoxic cells release more ROS than normal cells, studies indicate that under hypoxic conditions, the antioxidant defense network in hypoxic cells is more actively engaged, quickly diminishing ROS damage to tumor cells.[64] Additionally, the hypoxic conditions within tumors can stimulate the expression of hypoxia-inducible factor

HIF-1, which in turn promotes tumor cell proliferation and survival. This adaptation indirectly diminishes the effectiveness of radiotherapy.[65] Therefore, tissue hypoxia stands as one of the primary causes behind the failure of radiotherapy treatments. Combining radiation with pharmacological ROS inducers has become a focus of research. This section provides a brief summary of the combined treatment of radiation and CDT. CDT can increase the levels of ROS in the TME by catalyzing the formation of $^{\cdot}OH$ from H_2O_2, thereby killing tumor cells,[26] indicating that both can play a synergistic role in combating cancer. Various nanosystems have been developed that can be used not only for CDT but also for radiotherapy. Chen and colleagues synthesized a magnetic core–shell nanoplatform, Fe_3O_4@MnO_2. Manganese dioxide (MnO_2) as the shell layer reacts with intracellular glutathione to generate Mn^{2+}. In the presence of isoniazid (INH), Mn^{2+} decomposes hydrogen peroxide (H_2O_2) into hydroxyl radicals ($^{\cdot}OH$). Additionally, Fe_3O_4 can react with endogenous H_2O_2 to further damage tumor cells. Simultaneously, MnO_2 has the capability to catalyze the conversion of H_2O_2 into O_2, alleviating tumor hypoxia and enhancing radiotherapy efficacy. The CDT mediated by INH and Fe_3O_4@MnO_2 enhanced the therapeutic effect of radiotherapy *in vitro*, and *in vivo* experiments in Aicardi-Goutières syndrome tumor-bearing mice confirmed its good radiosensitizing effect.[66] Lin and colleagues created a nanocapsule containing near-infrared (NIR) fluorescent dye (IR1061) within gold-manganese oxide nanoparticles (JNP), which are also size-changeable, glutathione-responsive radiosenitizing nano-vesicles (JNP Ve). When exposed to glutathione (GSH), JNP Ve decomposes into gold nanoparticles (Au NPs) and manganese ions. Au NPs can generate ROS under X-ray irradiation and penetrate deeper into the tumor. Meanwhile, Mn^{2+} can induce CDT *via* a Fenton-like reaction, enhancing the efficacy of RT. *In vivo* experiments initially established a subcutaneous MCF-7 tumor-bearing mouse model for image-guided therapy, showing astonishing combined treatment effects, followed by the development of an *in situ* hepatocellular carcinoma mouse model that demonstrated JNP Ve's effective anti-tumor activity against deep-seated tumors.[67]

3.4 Mn-based CDT and starvation therapy

The sustained provision of nutrients and oxygen is crucial for the survival and proliferation of tumors. Interruption of oxygen supply can lead to hypoxia, cell damage, apoptosis, and necrosis. Angiogenesis induction is essential for tumor growth, and anti-angiogenesis treatment, a crucial part of starvation therapy (ST), is among the most effective clinical approaches to hinder tumor growth.[68] Employing CDT as a standalone treatment faces challenges, including the low catalytic efficiency of metal ions and the inadequate levels of endogenous H_2O_2. Similarly, using ST alone offers limited resistance to tumors. The "metal-oxidase" cascade catalytic system, which introduces cell metabolic oxidases into metal-based nanoplatforms, effectively resolves the limitations of both therapies individually. It supplies ample H_2O_2 and an appropriate acidic environment for CDT, further enhancing the synergistic impact with ST and thus bolstering anti-tumor efficacy.[69] For example, Xiao and colleagues constructed a multifunctional nanotherapeutic platform comprising manganese carbonate-deposited iron oxide nanoparticles (MCDION-Se) coated with nano-selenium (nano-Se). MCDION-Se releases a significant amount of Mn^{2+}, catalyzing the conversion of H_2O_2 into hydroxyl radicals ($^{\cdot}OH$) through Fenton-like reactions, effectively triggering cancer cell apoptosis. Moreover, the nano-Se on MCDION-Se substantially activates superoxide dismutase (SOD) within tumor tissues, facilitating the production of superoxide anion radicals (SOARs). Subsequently, SOD catalyzes SOARs to generate high levels of H_2O_2, further enhancing the efficiency of CDT. Simultaneously, nano-Se and Mn^{2+} inhibit the production of adenosine triphosphate (ATP), leading to starvation of cancer cells. Upon subcutaneous implantation of HeLa cells in BALB/c mice and subsequent intravenous administration, observations revealed that MCDION-Se treatment was effective and did not lead to resistance.[70]

3.5 Mn-based CDT and gas therapy

Gas therapy (GT), with its high efficacy, biocompatibility, and biosafety, has attracted widespread attention in nanomedicine. Gases employed in cancer treatment mainly encompass hydrogen, carbon monoxide (CO), hydrogen sulfide (H_2S), and nitric oxide (NO).[71,72] However, therapeutic gases are typically unstable and face challenges in precise accumulation and controlled release at tumor sites, leading to difficulties in direct administration or delivery clinically. Utilizing metal–organic frameworks (MOFs), known for their structural diversity and high surface areas, can effectively transport and release gases. Moreover, combining gas therapy with other treatments can synergistically enhance the efficacy of these therapies.[71–73] He *et al.* synthesized a biodegradable nanotherapeutic drug (MnS@BSA) that combines gas therapy and CDT. This nanoparticle is pH-responsive, releasing H_2S and Mn^{2+} under acidic conditions. The released H_2S is used for gas therapy, Mn^{2+} undergo a Fenton-like reaction to generate highly toxic $^{\cdot}OH$ for CDT, and a subcutaneous 4T1-Luciferase BALB/c mouse model is used to evaluate the anti-tumor effect and drug distribution of MnS@BSA through MRI and fluorescence imaging.[74] Zhao and team encapsulated manganese dioxide nanoparticles and carbonyl iron (FeCO) in mesoporous silica nanoparticles, creating a nanomedicine, FeCO–MnO_2@MSN, for combined CDT and gas therapy. Under the acidic pH of the TME, the disintegration releases ROS from MnO_2, and the produced $^{\cdot}OH$ further triggers the breakdown of FeCO into CO, causing damage to the DNA and mitochondria of cancer cells, thereby producing a synergistic anticancer effect both *in vitro* and *in vivo*. Additionally, the authors employed a 4T1 tumor-bearing mouse model for intravenous drug delivery, aligning with *in vitro* findings, which demonstrates the synergistic action between CDT and gas therapy.[75]

3.6 Mn-based CDT and photodynamic therapy

Photodynamic therapy (PDT) is a minimally invasive treatment approach that revolves around the interaction between

a photosensitizer, light of a specific wavelength, and molecular oxygen, selectively destroying tissues. After being injected into the body, the photosensitizer selectively accumulates in tumor tissues. Under exposure to light of a specific wavelength, the generated energy converts molecular oxygen into reactive oxygen, leading to the death of tumor cells.[76] PDT has the advantages of minimal side effects and low resistance. However, oxygen is a crucial raw material for inducing PDT, and the inherent hypoxia within the TME naturally inhibits the efficacy of PDT. To enhance tumor oxygenation or mitigate hypoxia, integrating PDT with other therapeutic strategies can be chosen for a synergistic approach.[77,78] The combination of chemotherapy and radiotherapy presents challenges like systemic toxicity, multidrug resistance, and complications.[79,80] Yet, when used in conjunction with CDT, enhancing oxygen concentration in tumor cells through the Fenton reaction and minimizing the distance between ROS and targets through mitochondrial targeting amplifies the effectiveness of PDT.[78] Wang and colleagues developed hollow-structured manganese carbonate nanoparticles encapsulating the photosensitizer (chlorin e6, Ce6), creating a responsive nanoplatform, H-$MnCO_3$/Ce6-PEG (HMCP NCs) (Fig. 2). HMCP NCs can upregulate intracellular ROS levels through two pathways. Firstly, Ce6 can generate singlet oxygen ($^1O_2$) under external laser irradiation, leading to photodynamic therapy (PDT). Secondly, $MnCO_3$ can specifically degrade into Mn^{2+} in the acidic TME and undergo a Fenton-like reaction, transforming endogenous H_2O_2 into $^{\cdot}OH$. Using an *in vivo* HeLa cell xenograft BALB/c mouse model, HMCP NCs demonstrated significantly enhanced therapeutic effects in inhibiting tumor growth without causing apparent damage to normal tissues.[81] To counteract the impacts of hypoxia and GSH depletion on the TME and the cellular antioxidant defense system, The biodegradable cancer cell membrane-coated mesoporous copper/silicon-manganese nanospheres (mCMSNs) designed by Liu *et al.* possess homotypic targeting ability for cancer cells. These nanospheres, under the synergistic influence of singlet oxygen ($^1O_2$) generated and ROS produced *via* a GSH-activated Fenton reaction, demonstrate outstanding combined CDT and PDT effects. Data from studies in *in vitro* and *in vivo* MCF-7 tumor-bearing nude mouse experiments show that under external laser irradiation, mCMSNs are capable of catalyzing the breakdown of endogenous H_2O_2 into O_2, ultimately generating toxic $^1O_2$, thereby alleviating the tumor hypoxic microenvironment. GSH induces the biodegradation of mCMSNs, releasing Cu^+ and Mn^{2+} ions to perform a Fenton-like reaction, achieving the consumption of GSH and the generation of $^{\cdot}OH$. Moreover, it unveils the capacity for specific recognition and homotypic targeting of cancer cells.[82]

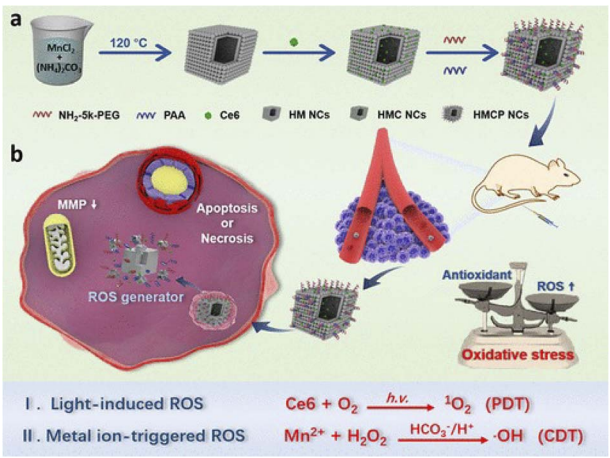

Fig. 2 (a) Synthetic procedure for HMCP NCs. (b) The scheme of dual-mode ROS-therapeutic mechanism of HMCP NCs for combined cancer treatment.[81] Copyright 2019, American Chemical Society.

3.7 Mn-based CDT and sonodynamic therapy

Sonodynamic therapy (SDT) is an innovative treatment approach that operates on a mechanism similar to photodynamic therapy (PDT). Its specific mechanism involves irradiating target tissues with ultrasound waves. Low-frequency focused ultrasound (US) enhances the target cells' uptake capacity by altering cell membrane permeability, sonoluminescence effect, and sonothermal effect, activating sonosensitizers to gain energy and causing electron transitions. As electrons return to their normal state, reactive oxygen species (ROS) are produced, effectively killing the target cells.[64,83] As nanomedicine progresses, there is an increasing emergence of new multifunctional sonosensitizers based on nanoparticles, encompassing strategies like multifunctional nano-sonosensitizing agents, comprehensive nanoplatforms, and combined therapeutic approaches. These new multifunctional nano-sonosensitizers typically consist of organic/inorganic agents capable of generating ROS, molecules modified to enhance blood-brain barrier permeability, tumor-specific drugs for accurate tumor localization, and metal ions to augment magnetic resonance imaging (MRI).[64,84] CDT demonstrates remarkable therapeutic outcomes and biosafety. Unlike conventional treatments, CDT can produce ROS[85] in a controlled manner regarding time and space, with unlimited penetration depth, targeting the high concentration of hydrogen peroxide (H_2O_2) in the TME. While SDT is capable of penetrating deep tissues, the hypoxic nature of the TME can constrain its therapeutic impact on tumors by diminishing the generation of ROS. The production of ROS is contingent upon the oxygen levels within the tumor.[86] The creation of Mn-based and other metal-ion nanoplatforms for the efficacy of CDT combined with SDT holds promising prospects and applications. Jiang and colleagues developed a $MnSiO_3$–Pt (MP) nanocomposite. $MnSiO_3$–Pt@BSA-Ce6 (MPBC), modified with bovine serum albumin (BSA) and chlorin e6 (Ce6), facilitates synergistic SDT and CDT (Fig. 3). Within this nanoplatform, the photosensitizer Ce6 can produce toxic singlet oxygen ($^1O_2$) under ultrasound irradiation. Meanwhile, platinum (Pt) loading can catalyze the decomposition of endogenously overexpressed H_2O_2 into O_2, overcoming tumor hypoxia and promoting the generation of $^1O_2$ induced by SDT. Moreover, MP can degrade in the TME to release Mn^{2+}, generating hydroxyl radicals ($^{\cdot}OH$) through Fenton-like reactions for use in CDT.[87] In order to overcome the issue of non-degradability associated with

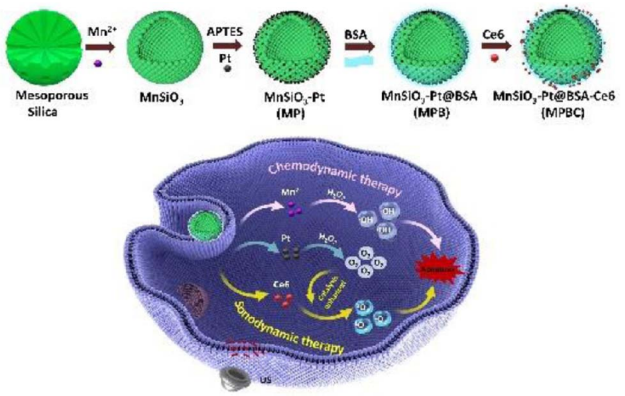

Fig. 3 Scheme of the synthesis process and therapeutic mechanism of MPBC nanoplatform.[87] Copyright 2022, Elsevier B. V.

traditional photosensitizers, Sun *et al.* developed a degradable perovskite-type manganese vanadate ($MnVO_3$) photosensitizer. Leveraging the inherent characteristics of perovskite, which include a narrow bandgap and abundant oxygen vacancies, $MnVO_3$ can undergo electron–hole separation and restricted recombination induced by US, thereby enhancing the quantum yield of ROS in SDT. Additionally, $MnVO_3$ can degrade under acidic conditions to produce manganese and vanadium ions, leading to a Fenton-like reaction to enhance CDT efficacy. The presence of high-valency vanadium in $MnVO_3$ enables it to deplete glutathione (GSH) within the TME, thus synergistically improving the therapeutic efficacy of both SDT and CDT. Crucially, the perovskite structure confers excellent biodegradability upon $MnVO_3$, mitigating the prolonged presence of residuals in metabolic organs after treatment. Based on these characteristics, *in vivo* experiments in 4T1 tumor-bearing mice observed that US-assisted $MnVO_3$ achieved good anti-tumor effects with lower systemic toxicity,[88] perfectly combining the advantages of SDT and CDT treatments.

3.8 Mn-based CDT and photothermal therapy

Photothermal therapy (PTT) is a non-invasive treatment approach that uses photothermal conversion nanomaterials exposed to near-infrared (NIR) light irradiation to target tumor sites, converting light energy into thermal energy to kill tumor cells.[89] Unlike radiotherapy, PTT can kill cancer cells without damaging nearby normal cells. Due to its affordability, high efficacy, minimal invasiveness, limited side effects, and precise targeting capabilities, it has attracted widespread attention in cancer treatment.[91] By using selective photothermal absorbers, minimally invasive targeted treatment of tumors that are otherwise challenging to address. All laser transmission modes aim to uniformly elevate the temperature within tumor tissues, ensuring that surrounding healthy tissues remain unharmed. For effective tumor cell ablation, photothermal damage generally occurs when the center of the tumor temperature exceeds 50 °C, creating a temperature gradient that brings the edges of the tumor to the therapeutic temperature.[92] A primary concern with PTT is that overheating in the tumor area might cause undue harm to normal tissues and potentially lead to resistance. Moreover, the limited depth of light penetration could mean insufficient ablation of malignant tumors beyond the irradiated region.[93] Therefore, improving PTT therapy is where promising therapeutic explorations are currently directed. While manganese-based nanostructures show potential as agents for CDT, their capability for photothermal conversion is yet insufficient to serve as ideal agents for combined therapy. Ma *et al.* developed a bifunctional $Bi_{2-x}Mn_xO_3$ nanoplatform for synergistic PTT/CDT treatment of tumors. Doping a small amount of bismuth (Bi) into the structure has altered the photothermal and CDT properties of $Bi_{2-x}Mn_xO_3$, thus enhancing photothermal conversion efficiency and hastening the production of $^{\cdot}OH$. The presence of reductive Mn^{4+} contributes to disrupting the internal redox balance in tumors by increasing the consumption of GSH, thereby improving the effectiveness of CDT. At the same time, a moderate photothermal effect, induced by laser irradiation, can further expedite GSH depletion and $^{\cdot}OH$ generation in the tumor vicinity, thus augmenting the CDT impact. An evaluation of combined treatment effects using a 4T1 tumor-bearing BALB/c mouse model revealed that the CDT/PTT synergistic treatment group showed the most favorable results.[94] Moreover, Chen *et al.* constructed a stable spherical nanostructure based on polyethylene glycolated manganese-doped polydopamine (PDA), PEG-PDA@Mn (PP@Mn NPs) (Fig. 4). PP@Mn NPs can trigger PTT under NIR light, with the released Mn^{2+} undergoing Fenton-like reactions to induce CDT effects. In combination with PTT, they generate abundant ROS causing ferroptosis, and T_1-weighted signal enhancement-mediated MRI phenomenon is also observed *in vivo* in MFC tumor-bearing mice.[90]

3.9 Mn-based CDT and immunotherapy

Clinically, immunotherapy is a treatment that either suppresses or activates the immune system to treat diseases. In the context of cancer, immunotherapy aims to bolster the immune response against cancer cells. Generally, the former involves systemic administration of cytokines, cancer vaccines, or adoptive cell transfer, and the latter pertains to regulating the immunosuppressive TME.[95] Immunotherapy is progressively recognized as the standard approach for treating various types of locally advanced and metastatic human cancers. However, the overall response rate of patients to immunotherapy is still not ideal, and combining multiple immunotherapy drugs to enhance therapeutic effects often leads to higher toxicity. Consequently, nanomaterials can act as scaffolds or carriers, amalgamating multiple drugs or treatment modalities while concurrently managing various immunoregulatory pathways, thereby minimizing side effects.[96] Mn-based nanomaterials possess a variety of functions that augment tumor immunotherapy. They are capable of directly activating cyclic GMP-AMP (cGAMP) synthase (cGAS), triggering the noncanonical catalytic synthesis of 2′,3′-cGAMP and activating the stimulator of interferon genes (STING). Consequently, manganese-based nanomaterials demonstrate significant potential in bolstering immune responses. They aid in facilitating antigen uptake,

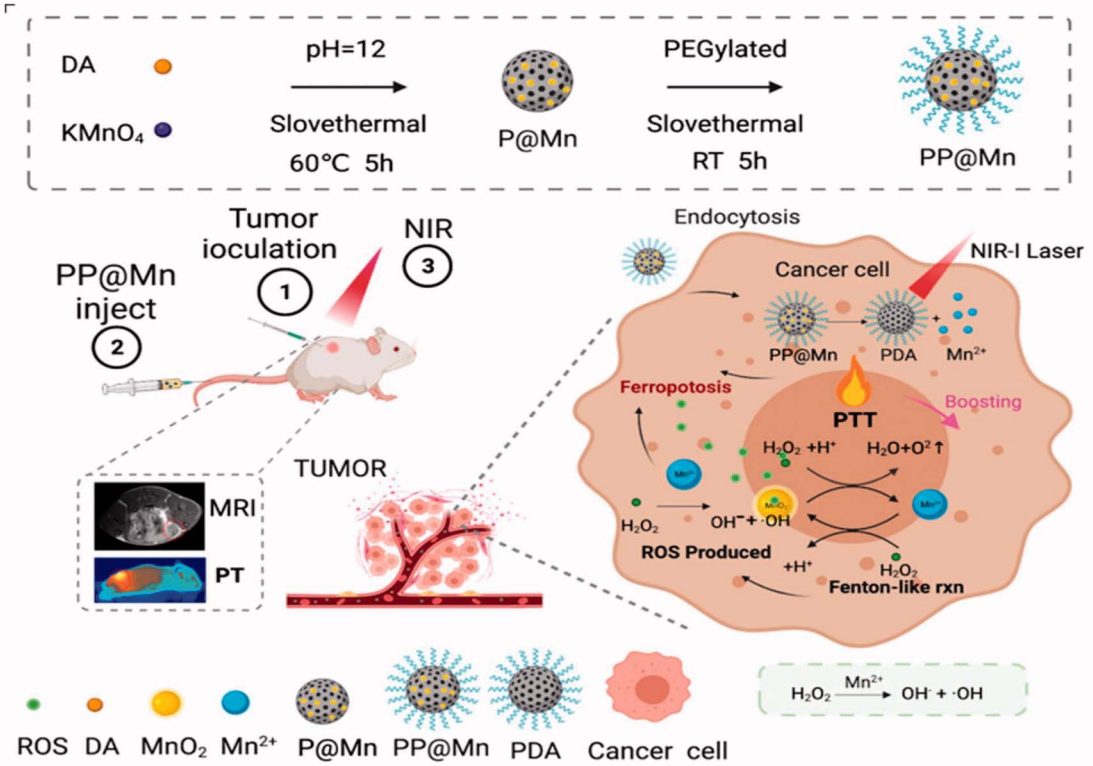

Fig. 4 Scheme of the synthesis process and therapeutic mechanism of PP@Mn.[90] Copyright CCBY, 2022, Informa UK Limited.

presentation, and the formation of germinal centers. This multifaceted action renders them effective adjuvants for immunotherapy, leveraging the body's immune system to target and eliminate tumor cells more efficiently.[97] In tumor immunotherapy, manganese-based nanomaterials can function as biocompatible nanocarriers for the delivery of immunotherapeutic agents, activating the host's immune system. Additionally, they can serve as adjuvants to adjust the tumor immune microenvironment, foster immune responses, and activate the cGAS-STING pathway, thereby initiating tumor immunotherapy.[98] Combining systemic or local immunotherapy with traditional clinical methods has shown considerable significance in the treatment of cancer. Chen and colleagues constructed a nanocomposite based on Mn^{2+} and cytosine–phosphate–guanine oligodeoxynucleotides (CpG ODN) (MnCpGPNCs). MnCpGPNCs release Mn^{2+} within tumor cells to initiate Fenton-like reactions that generate ROS and induce cell apoptosis. They also amplify the activation of the interferon gene pathway, leading to increased production of type I interferons, which in turn prompts a response from various immune cells. Moreover, CpG ODN acts as an immunological adjuvant to bolster antigen presentation and the potency of immune induction. Binding of Mn^{2+} is shown to boost the CDT effect of immunotherapy. In a bilateral CT26 tumor xenograft mouse model, MnCpGPNCs were observed to effectively suppress both primary and distant tumors and prevent the onset of tumors.[99] Interestingly, Deng *et al.* developed a calcium–manganese dual-ion hybrid nanostimulator (CMS), which enhances anti-tumor immunity by inducing ferroptosis and awakening innate immunity, and can also serve as an immunological adjuvant for triple-negative breast cancer (TNBC). Manganese within CMS contributes to GSH depletion and engages in Fenton-like reactions to generate ROS, and the alteration of its mixed valence states can also lead to the occurrence of ferroptosis. Interestingly, CMS serves as an immune adjuvant that awakens innate immunity by mitigating tumor hypoxia and activating the Mn^{2+}-induced STING signaling pathway. This process can lead to the infiltration of tumor-specific cytotoxic T lymphocytes (CTLs) into tumor tissues. In bilateral 4T1 tumor-bearing BALB/c mice, a significant inhibitory effect on distant tumors was observed, demonstrating the achievement of an anti-tumor immune response.[100]

3.10 Mn-based CDT-involved other multimodal synergistic therapy

The use of a single therapeutic modality is inadequate for effective tumor cell eradication.[101] Leveraging the synergistic interplay between tumor chemodynamic therapy and two other treatment modalities allows for the optimal therapeutic outcome with the least dosage, thereby minimizing adverse effects, compared to each therapy used alone. The tri-modal synergistic therapy can be accomplished by amalgamating different therapeutic agents in one nanoparticle platform.

For instance, Wang *et al.* developed a SSMID (Se@SiO_2@-MnO_2-ICG/DOX) nanocomposite (NCs) for tri-modal synergistic therapy of chemotherapy/photothermal/chemodynamic, useable for magnetic resonance imaging (Fig. 5A). SSMID

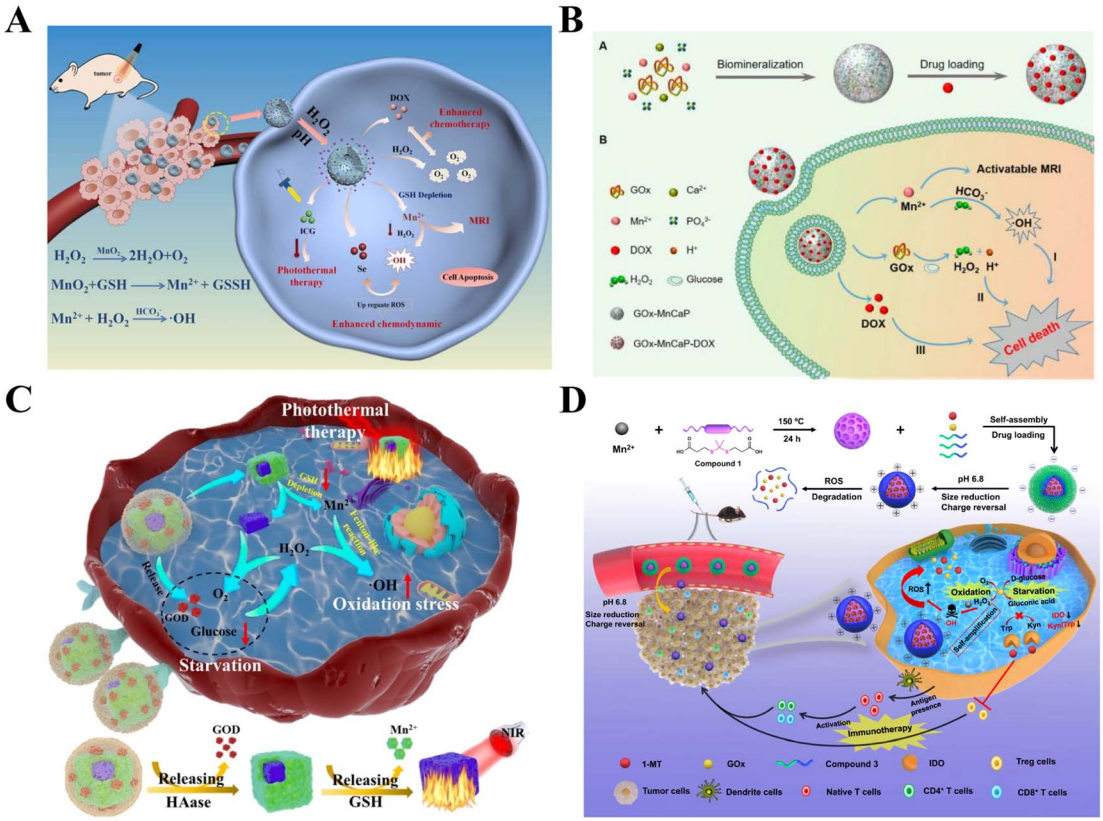

Fig. 5 Schematic diagram of multimodal therapy of manganese-based nanomaterials: (A) scheme of the synthesis process and therapeutic mechanism of SSMID NCs;[102] copyright 2022, Elsevier B. V. (B) Schematic illustration of GOx-MnCaP-DOX applied for MRI-monitored cooperative cancer therapy;[104] copyright 2019, American Chemical Society. (C) Scheme of the therapeutic mechanism of PBMO-GH;[105] copyright 2021, Elsevier B. V. (D) Construction of PCP-Mn-DTA@GOx@1-MT and its immune stimulation capabilities.[106] Copyright CCBY, 2022, Springer Nature.

specifically disintegrates in the TME with mild acidity, high H_2O_2, and overexpressed GSH, subsequently liberating Mn^{2+}, doxorubicin (DOX), and selenium (Se). The components within such a tri-modal therapeutic nanoparticle platform each play a distinct role in safeguarding normal tissues while targeting tumor cells through CDT and chemotherapy. MnO_2 reacts with GSH and H_2O_2 to produce O_2 and Mn^{2+}, alleviating tumor hypoxia to bolster the efficacy of chemotherapy, and consuming GSH to enhance the oxidative stress of CDT. More importantly, the released indocyanine green (ICG) can mediate the effect of photothermal therapy (PTT) under NIR laser irradiation, achieving enhanced PTT/CT/CDT tri-modal therapy in conjunction with Mn^{2+} and DOX. The authors evaluated the therapeutic efficacy using an A549 tumor-bearing mouse model, finding both the anti-tumor effect and the degradation metabolism to be favorable.[102] As Mn-based nanomaterials are involved in oxygen production and GSH depletion, they are closely linked to ROS generation and GSH consumption, substantially augmenting the effectiveness of oxygen-reliant PDT or SDT.[103] Guan and his team created a biodegradable nanocomposite (mZMD) using a mesoporous zeolitic imidazolate framework loaded with MnO_2 and doxorubicin hydrochloride to facilitate synergistic SDT/CDT/chemotherapy. This effect is attained by augmenting oxidative stress and circumventing multidrug resistance mechanisms. Upon US irradiation, mZMD nanoparticles decompose within the TME. The decomposed manganese dioxide undergoes glutathione oxidation reactions to enhance oxidative stress. The O_2 produced during this process serves to alleviate the hypoxic conditions of the TME, thereby enhancing the effect of SDT/chemotherapy. Concurrently, the generated Mn^{2+} undergoes Fenton-like reactions to yield $^{\bullet}OH$ for CDT and serves as a T_1-weighted MRI contrast agent. Moreover, the released Zn^{2+} engage in additional redox reactions within the TME. Along with the ROS generated, these actions work to suppress the expression of P-glycoprotein (P-gp), a key factor in the development of multidrug resistance, thereby overcoming one of the major hurdles in effective cancer treatment. Finally, *in vivo* experiments on HeLa tumor-bearing nude mice confirmed that mZMD has an excellent inhibitory effect on tumors under the action of US.[107]

Besides, the combined treatment involving CDT, starvation therapy, and other modalities has recently emerged as a prominent research focus. Fu *et al.* ingeniously utilized an innovative *in situ* biomimetic mineralization technique to encapsulate glucose oxidase (GOx) within Mn-doped calcium phosphate (MnCaP) nanoparticles, also incorporating the chemotherapeutic agent doxorubicin (DOX), constructing a spherical nanoparticle (Fig. 5B). This nanoparticle features

biodegradability, strong biocompatibility, and TME pH sensitivity. GOx can consume glucose within the tumor to achieve a "starvation" effect, while the released Mn^{2+} can mediate Fenton-like reactions to convert H_2O_2 into highly toxic hydroxyl radicals, achieving the purpose of CDT, and the production of gluconic acid increases the acidity of the TME, further promoting the degradation of the nanoparticle platform and enhancing CDT. This study demonstrated that GOx-MnCaP loaded with the anticancer drug DOX could combine ST, Mn^{2+}-mediated CDT and DOX-induced chemotherapy to treat 4T1 tumor-bearing mice demonstrating a substantial increase in therapeutic efficacy compared to each single therapy.[104] Wang and others proposed embedding carbonyl manganese (MnCO) into Zr(IV)-based metal–organic frameworks (MOFs), designing a H_2O_2-triggered CO gas release nanoplatform. GOx is loaded into the porous structure of MOFs, not only the transformation of intracellular glucose into H_2O_2, effectively severing the energy supply to cancer cells. And the Mn^{2+} generated by MnCO undergoes a reaction with intracellular H_2O_2, producing cytotoxic $^{\bullet}OH$, which induces apoptosis of cancer cells and expedites the release of CO and energy expenditure. The use of HeLa tumor-bearing nude mice for *in vivo* experiments revealed that this multifunctional nanoplatform effectively inhibited tumor growth *via* a synergistic effect, thus proving its capability to introduce a novel approach for integrating starvation, gas, and chemodynamic therapies within a single material.[108] Additionally, Gu *et al.* investigated the efficacy of combined treatment with starvation therapy, CDT, and photothermal therapy (Fig. 5C). They created a tumor-targeting nanoparticle platform (PBMO-GH) by adsorbing manganese dioxide (MnO_2) and glucose oxidase (GOD) onto Prussian Blue (PB). The enzymatic reaction catalyzed by GOD generates H_2O_2 and gluconic acid. Simultaneously, PB can catalyze H_2O_2 to produce oxygen, continuously consuming glucose to achieve ST, and its photothermal conversion properties enable PTT under NIR light. The Mn^{2+} generated from the reaction between MnO_2 and GSH can amplify CDT by producing highly toxic $^{\bullet}OH$ through Fenton-like reactions.[105] As GOx has an immune-stimulating effect, it can not only effectively eliminate tumor cells by competitively consuming glucose and producing cytotoxic ROS, but also exposes tumor-associated antigens (TAAs), leading to a comprehensive antitumor effect, and a favourable therapeutic effect is observed after intravenous administration of MDA-MB-231 in tumor-bearing mice.[109] Dai and colleagues developed a pH and ROS dual-sensitive degradable nanosystem for CDT/starvation therapy/immunotherapy, which can co-deliver glucose oxidase (GOx) and 1-methyltryptophan (1-MT) (PCP-Mn-DTA@GOx@1-MT) (Fig. 5D). The highly ROS-sensitive degradable MOF nanoreactor can rapidly decompose within ROS-rich tumor cells, releasing Mn^{2+}, GOx, and 1-MT. This minimizes the long-term retention toxicity of traditional MOFs. The released GOx continuously consumes glucose to promote H_2O_2 production and generate highly toxic $^{\bullet}OH$ through Mn^{2+}, leading to the complete degradation of MOF and drug release, thereby enhancing the therapeutic effect; and it also can enhance tumor immune response and immune memory, alleviates tumor immune tolerance, synergistically increasing the effectiveness of immunotherapy. The assessment of anti-tumor immune responses and treatment outcomes using both B16-F10 and 4T1 tumor-bearing mouse models showed uniformly positive anti-tumor therapeutic effects.[106]

In conclusion, relying solely on manganese (Mn) for CDT does not yield optimal therapeutic outcomes, to enhance the effectiveness of tumor treatments and simultaneously reduce both dosage and side effects, a significant number of Mn-based nanomaterials have been recently developed to be used in conjunction with other therapeutic drugs, facilitating the synergy of CDT with other multimodal treatments (Table 1). Future developments will also focus on a broader range of multimodal synergistic treatments associated with CDT, aiming to accomplish personalized treatment of tumors.

4 Mn-based nanotheranostics for imaging-guided CDT

The Magnetic Resonance Imaging (MRI) guidance capability of manganese-based nanomaterials, when combined with other imaging modalities, holds broad prospects. Combining Mn-based nanomaterials with other imaging agents (CAs) enables MRI-based multimodal imaging-guided CDT. MRI has the capability to visualize the pathophysiological hypoxic microenvironment and oxygenation status at tumor sites. This not only contributes to the early detection of tumors but also provides real-time monitoring during the treatment of tumors.[110]

4.1 Solely MRI-guided CDT

Manganese-based nanomaterials possess superior MRI capabilities and are widely used for detecting *in vivo* drug distribution, monitoring the tumor treatment process, and evaluating tumor treatment outcomes. Lin and others constructed mesoporous silica nanoparticles coated with MnO_2 ($MS@MnO_2$ NPs). This study was the first to demonstrate that manganese dioxide can deliver Mn^{2+} and deplete GSH. The MnO_2 shell engages in redox reactions with glutathione, producing Mn^{2+} and glutathione disulfide (GSSG). The abundant HCO_3^-/carbon dioxide (CO_2) buffer in physiological culture media supports the Mn^{2+}-catalyzed production of $^{\bullet}OH$. When the nanoparticles are internalized into tumor cells, the MnO_2 shell can decompose, producing Mn^{2+}, which undergoes Fenton-like reactions to generate highly toxic $^{\bullet}OH$, and deplete intracellular GSH to inhibit the clearance of $^{\bullet}OH$. Concurrently, the dissociation of the MnO_2 shell in response to GSH depletion can also act as a regulatory mechanism for MS NPs, controlling the release of encapsulated drugs. Compared to MnO_2, Mn^{2+} has a higher longitudinal (T_1) relaxivity, with data showing a 12.8-fold increase in the r_1 value after GSH treatment. After intratumoral injection in U87MG tumor-bearing mice, the MnO_2 shell can display the GSH-activated MRI contrast effect, which can be used to monitor the reaction between MnO_2 and GSH, as well as the CDT process.[111] Su *et al.* employed microfluidic chip technology to encapsulate doxorubicin (DOX) within manganese alginate nanogels, resulting in the formation of DOX@Mn-Alg. DOX@Mn-Alg facilitates the maturation of dendritic cells (DC)

Table 1 Summary of manganese-based chemodynamic therapy in synergy with multimodal treatment on nanoplatforms

Therapies	Materials	Therapeutic mechanisms	Tumor model	Administration	Ref.
Chemodynamic therapy and chemotherapy	TPP-DOX@MnBSA	Mn^{2+} increases intracellular highly toxic $^{\bullet}OH$, while DOX is used in chemotherapy. Of tumor metastasis	4T1 and MCF-7 mouse tumor xenograft, MCF-7 transgenic zebrafish tumor xenograft	Intravenous injection, transgenic zebrafish are injected under a microscope	56
Chemodynamic therapy and radiotherapy	Combined use of Fe_3O_4@MnO_2 and INH	Both MnO_2 and Fe_3O_4 can react with endogenous H_2O_2 to produce highly toxic $^{\bullet}OH$. The generated O_2 relieves hypoxia and improves the effect of radiotherapy	AGS tumor xenograft	Intravenous injection	66
	Au–MnO Janus NPs nanovesicles	Au NPs generate reactive oxygen species under X-ray irradiation, and Mn^{2+} undergoes a Fenton-like reaction to generate reactive oxygen species, which jointly enhance the RT effect	Orthotopic liver tumor and MCF-7 tumor xenograft	Intravenous injection	67
Chemodynamic therapy and starvation therapy	Nanoselenium-coated manganese carbonate-deposited iron oxide nanoparticle (MCDION-Se)	Mn^{2+} undergoes a Fenton-like reaction to generate $^{\bullet}OH$, and nano-Se activates SOD to catalyze SOARs to generate H_2O_2, both of which inhibit the production of ATP	HeLa tumor xenograft	Intravenous injection	70
Chemodynamic therapy and gas therapy	MnS@BSA	H_2S is released for gas therapy, while Mn^{2+} generates highly toxic $^{\bullet}OH$ for CDT	4T1 tumor xenograft	Intravenous injection	74
	FeCO-MnO_2@MSN	MnO_2 generates $^{\bullet}OH$, FeCO generates CO, and ROS and CO can damage the DNA and mitochondria of cancer cells respectively	4T1 tumor xenograft	Intravenous injection	75
Chemodynamic therapy and photodynamic therapy	H-$MnCO_3$/Ce6-PEG (HMCP NCs)	Ce6 generates singlet oxygen ($^1O_2$) under external laser irradiation, causing PDT, while $MnCO_3$ degrades into Mn^{2+} produce highly toxic $^{\bullet}OH$	HeLa tumor xenograft	Intravenous injection	81
	Cancer cell membrane-coated mesoporous copper/manganese silicate nanospheres (mCMSNs)	mCMSNs catalyzes the decomposition of endogenous H_2O_2 into O_2, producing toxic $^1O_2$, and GSH triggers the biodegradation of mCMSNs to produce Cu^+ and Mn^{2+}, producing $^{\bullet}OH$	MCF-7 tumor xenograft	Intravenous injection	82
Chemodynamic therapy and sonodynamic therapy	$MnSiO_3$-Pt@BSA-Ce6 (MPBC)	Ce6 generates $^1O_2$ under US irradiation. Pt catalyzes the decomposition of endogenous H_2O_2 to generate oxygen, promotes the generation of $^1O_2$ induced by SDT, and Mn^{2+} generates hydroxyl radical $^{\bullet}OH$	U14 tumor xenograft	Intratumoral injection	87
	$MnVO_3$	$MnVO_3$ enhances the quantum yield of ROS. Mn^{2+} and vanadium ions can consume GSH and produce Fenton-like reaction	4T1 tumor xenograft	Intravenous injection	88
Chemodynamic therapy and photothermal therapy	$Bi_{2-x}Mn_xO_3$ (BM)	BM has improved light heat conversion efficiency in near infrared, and the reduction of the local temperature of the restore Mn^{2+} and the local temperature of the tumor area will increase the consumption of endogenous GSH, thereby enhancing the CDT effect	4T1 tumor xenograft	Intratumoral injection	94
	PEG-PDA@Mn (PP@Mn NPs)	PDA can be used for tumor PTT, Mn^{2+} causes Fenton reaction to cause CDT	MFC tumor xenograft	Intravenous injection	90
Chemodynamic therapy and immunotherapy	MnCpGPNCs	MnCpGPNCs release Mn^{2+}, promoting the stimulation of the STING pathway, increasing the production of IFN-I to increase the immune effect, CpG ODNs, as an immune agent enhanced antigen presentation and immune induction effect	Unilateral/bilateral CT26 tumor xenograft	Intravenous injection	99
	Ca & Mn dualion hybrid nanostimulator (CMS)	Mixed-valence manganese can deplete GSH and generate ROS. Exogenous Ca^{2+} induces mitochondrial Ca^{2+} overload, GPX4 loss and LPO lead to ferroptosis	Bilateral 4T1 tumor xenograft	Intratumoral injection	100
	Se@SiO_2@MnO_2 -ICG/DOX		A549 tumor xenograft	Intravenous injection	102

Table 1 (*Contd.*)

Therapies	Materials	Therapeutic mechanisms	Tumor model	Administration	Ref.
Chemodynamic therapy, chemotherapy and photothermal therapy		It simultaneously acts as PTT under NIR laser irradiation, promoting the release of Mn^{2+} and DOX, MnO_2 reacts with GSH and H_2O_2 to generate O_2 and Mn^{2+}, alleviating tumor hypoxia and initiating CDT			
Chemodynamic therapy, chemotherapy and sonodynamic therapy	Mesoporous zeolitic-imidazolateframework@MnO_2/doxorubicin hydrochloride (mZMD)	MnO2 can oxidize glutathione, catalyze H_2O_2 to produce O_2. Mn^{2+} can generate $^{\bullet}OH$, inducing CDT, and Zn^{2+} can collaboratively inhibit the expression of P-glycoprotein with generated ROS to overcome drug resistance	HeLa tumor xenograft	Intravenous injection	107
Chemodynamic therapy, chemotherapy and gas therapy	DOX-loaded GOx-MnCaP nano-therapeutic agent	Gox is a cofactor of starvation therapy. Mn^{2+}-mediated Fenton-like reaction converts to highly toxic hydroxyl radicals for CDT, while DOX induces chemotherapy	4T1 tumor xenograft	Intratumoral injection	104
Chemodynamic therapy, starvation therapy and gas therapy	Glucose oxidase (GOx) and carbonyl manganese (MnCO) are encapsulated within UiO-67-bpy	GOx accelerates CO release and energy consumption. Mn^{2+} generated by MnCO can form cytotoxic $^{\bullet}OH$ through a Fenton-like reaction	HeLa tumor xenograft	Intravenous injection	108
Chemodynamic therapy, starvation therapy and photothermal therapy	GOD is loaded onto an adsorbed MnO_2 Prussian blue (PB) nanoplatform (PBMO-GH)	GOD and PB can catalyze H_2O_2 promote glucose consumption for starvation therapy, PB can achieve PTT under NIR light. The Mn^{2+} generated from the reaction of MnO_2 can produce highly toxic $^{\bullet}OH$	MDA-MB-231 tumor xenograft	Intravenous injection	105
Chemodynamic therapy, starvation therapy and immunotherapy	PCP-Mn-DTA@GOx@1-MT	GOx consumes glucose and generates ROS, inducing drug release. Its activation of tumor starvation and recruitment of enhance immune response and stimulate immune memory, while effectively relieving immune tolerance by blocking Ido	B16-F10 and 4T1 tumor xenograft	Intravenous injection	106

and enhances tumor infiltration by $CD8^+$ T cells, effectuating immunotherapy. It also disintegrates within tumor cells due to the acidic pH of the TME, releasing DOX to kill tumor cells. The liberated Mn^{2+} participates in the Fenton reaction, consistently supplying H_2O_2 to form highly toxic $^{\bullet}OH$, and the measured T_1 relaxivity of DOX@Mn-Alg reached 9.614 mM^{-1} s^{-1}, providing enhanced T_1-weighted MRI contrast for diagnostics in CT26 tumor-bearing mice.[112] An *et al.* crafted a multimodal nanomaterial, Mn-Ti_3C_2@PEG, for MRI-guided thermal ablation and CDT. Based on linear fitting, the r_1 value of Mn-Ti_3C_2@PEG was calculated to be 1.05 mM^{-1} s^{-1}, indicating that the magnetic properties of the Mn component can make it serve as a T_1-weighted contrast agent for MRI with good imaging effects in reality. Additionally, it can generate highly toxic $^{\bullet}OH$ through a Fenton-like reaction, and given MXene's high photothermal conversion capability and photothermal stability, it can effectively inhibit tumor growth through PTT, realizing synergistic therapy with PTT/CDT dual modes. The construction of 4T1 tumor-bearing mice and the observation of their MRI and photothermal imaging indicated favorable anti-tumor treatment outcomes.[113]

4.2 Dual-modality imaging-guided CDT including MRI

Multi-responsive nanoprobes hold great promise in biomedical imaging applications, characterized by their low background and high sensitivity. Mn-based nanomaterials offer the capability for multimodal imaging by incorporating different imaging agents (CAs). Integrating different imaging techniques allows for the monitoring of distinct cellular and tissue states throughout tumor therapy. Modalities like positron emission tomography (PET) can assess tumor hypoxia.[110] Fluorescence imaging (FI) is suitable for applications like vascular imaging, neural imaging, and cell tracking. Tracking tumor cells facilitates the understanding of their metastasis and aids in surgical interventions; and photoacoustic imaging can effectively perform structural and functional imaging of biological tissues, and can be used for early detection and treatment monitoring of cancer. Combining manganese-based nanomaterials with fluorescence groups can achieve MRI/FI. For example, Li and others labeled indocyanine green (ICG) on manganese metal–organic framework (MOF) nanoparticles (NPs), simultaneously loading SiOUM1, siPTPRZ1, and cisplatin, and linking with arginine–glycine–aspartic acid (RGD) peptide. This realizes targeted therapy mediated by siRNA

interference, enhancing cisplatin treatment and CDT. When injected into subcutaneous OCM1-tumor-bearing BALB/c nude mice, this nanomaterial enables the observation of time-dependent biodistribution and a lung metastasis model in the tumor-bearing mice *via* bioluminescence imaging (Fig. 6). And the FI capability facilitates the real-time monitoring of its *in vivo* distribution. This nanosystem provides an approach for precision drug delivery in treating tumors, endowed with dual-modal imaging capabilities.[55] Numerous studies have proven the application of PT imaging. Zhu and others constructed a multifunctional intelligent nanoparticle platform MnFe-LDH/MTX@GOx@Ta (MMGT) for MRI/photothermal (PT) dual-modal imaging-guided CDT/chemotherapy dual-modal therapy, with self-supplied H_2O_2 and enhanced photothermal effects. Through a simple hydrothermal reaction, MnFe-LDH (M) was synthesized and subsequently loaded with the methotrexate (MTX). Then, glucose oxidase (GOx) and tannic acid (Ta) are modified separately to assemble MMGT. MMGT degrades within the tumor microenvironment to generate Mn^{2+}/Fe^{3+}, GOx, and MTX. Mn^{2+}/Fe^{3+} and MTX are capable of transforming endogenous H_2O_2 into $^{\bullet}OH$ *via* the Fenton reaction and chemotherapy, facilitating combined CDT. Furthermore, *in vitro* experiments demonstrated that in PBS solution at pH 5 with 10 mM glucose, the MMGT r_1 value increased to 1.24 mM^{-1} s^{-1}, indicating that Mn^{2+} enhances the T_1-MRI contrast signal. And the released GOx was able to consume glucose and provide H_2O_2, thereby alleviating constraints on CDT. MnFe-LDH is capable of transforming NIR light energy into thermal energy, facilitating PT imaging and simultaneously boosting the efficacy of CDT. After intravenous injection, the PT imaging results showed the temperature changes of the tumor at different time points, the T_1-weighted MR images revealed that MMGT accumulated in the tumor tissue and successfully degraded into Mn^{2+}, with a good contrast effect.[114]

Gold nanoparticles (AuNPs) can serve not only as photoacoustic imaging agents and are widely used in long-term computed tomography (CT) scan. Combining manganese-based nanomaterials with Au NPs can also easily achieve MRI/CT. Sha *et al. in situ* doped metal manganese onto gold core mesoporous silica nanoparticles to create Au@MMSN. Following this, they further modified Au@MMSN with sodium alendronate (Ald), and loading doxorubicin (DOX) onto Au@MMSN-Ald, it demonstrated effective osteosarcoma targeting capabilities. The resultant DOX@Au@MMSN-Ald possesses dual-modal CT/MR imaging capabilities and features combined chemotherapy/CDT properties. Hence, in certain TME, DOX@Au@MMSN-Ald releases gold nanoparticles from the core and Mn^{2+} from the shell, which are respectively validated in CT and MR dual-modal imaging, evidencing the efficient accumulation of Au@MMSN-Ald at tumor locations. The manganese ions and DOX can mediate CDT and chemotherapy respectively. Intratumoral injection of DOX@Au@MMSN-Ald *in situ* 143B tumor-bearing mice can clearly display tumor site images, while intravenous administration allows for tracking of Mn^{2+} release and monitoring of the *in vivo* CDT process. All in all, the producted DOX@Au@MMSN-Ald nanoparticles, with their imaging guidance and combined treatment advantages, also exhibited excellent therapeutic effects in eliminating cancer cells and inhibiting osteosarcoma growth.[115]

4.3 Multimodal imaging-guided CDT including MRI

In the pursuit of improved imaging precision, precise diagnostics, and enriched information, integrating Mn-based nanomaterials with multifunctional nanoprobes for tumor multimodal imaging-guided CDT is effective. NIR-II semiconductor polymers are excellent photothermal agents capable of effectively absorbing NIR-II light and converting it into thermal energy to mediate PTT and kill tumor cells. This NIR-II absorption capability can be utilized to achieve efficient PTT guided by NIR-II photoacoustic imaging. Utilizing this feature, Dai and colleagues engineered NIR-II phototherapeutic nano-

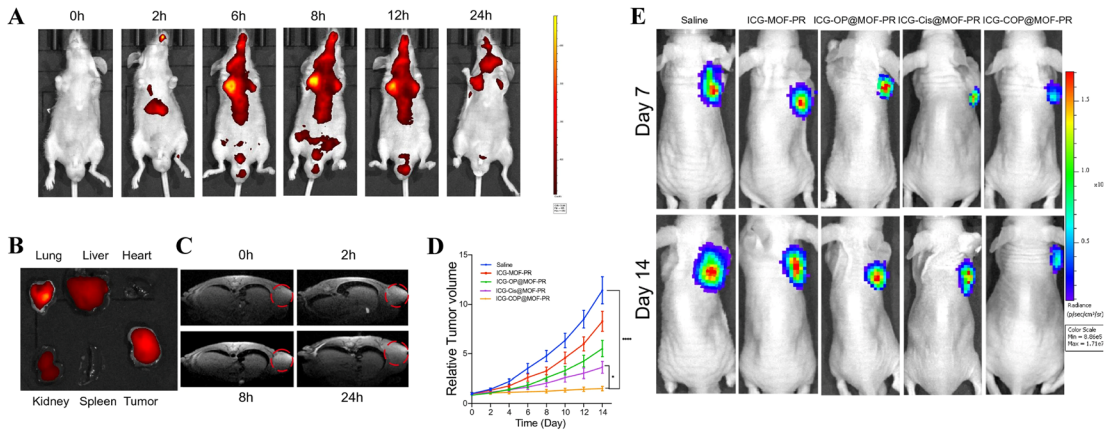

Fig. 6 Pharmacokinetics and targeting effect and tumor suppression effects of intravenously injected NPs *in vivo*. (A) *In vivo* real-time bioluminescence imaging of UM tumor-bearing mice at different time points after administration of ICG-COP@MOF-PR; (B) ICG fluorescent intensities from ex vivo imaging of the major organs, and the tumors 24 h after injecting ICG-COP@MOF-PR; (C) T_1-weighted MRI after intravenous injection with ICG-COP@MOF-PR at predesigned time points; (D and E) the tumor growth curves and bioluminescence imaging showed UM growth with different treatments *in vivo*.[55] Copyright CCBY, 2023, Springer Nature.

adjuvants (PMR NAs) by coordinating Mn^{2+} with ultrasmall NIR-II semiconductor polymer dots and toll-like receptor agonists (R848). PMR NAs disintegrate in response to the acidic TME, and the disintegrated ultrasmall NIR-II semiconductor polymers synergize with laser irradiation for PTT within the tumor and can be used for PT imaging, with their inherent fluorescence allowing for FI as well. The released Mn^{2+} can mediate a Fenton-like reaction to induce CDT. Its T_1-weighted MR signal was observed to increase with concentration, yielding an r_1 value of 5.68 mM^{-1} s^{-1}, thereby enhancing the MRI effect (Fig. 7). The synergistic therapy of CDT/PTT can induce anti-tumor immunity through the ICD effect and, in conjunction with the simultaneously released R848, enhances the anti-tumor immune response. *In vivo* experiments using the B16F10 bilaterally tumor-bearing mice model to validate the anti-tumor effect demonstrated that PMR NAs have a multilevel tumor-killing effect, which can be used for precise diagnosis of deep-seated tumors and amplification of anti-tumor immunotherapy.[116] The integration of fluorescent molecules is a widely recognized strategy for multimodal imaging, an approach also employed by Cheng and others, they consistently integrated Mn^{2+}, MnO_2, and the photosensitizer indocyanine green (ICG) onto Cu/Zn-metal–organic frameworks (MOF), culminating in the formation of ICG@Mn/Cu/Zn-MOF@MnO_2. Cu^{2+} and MnO_2 reacted with GSH to reduce ROS depletion and produce Mn^{2+} that mediates MRI and was calculated to have an r_1 value of 7.91 mM^{-1} s^{-1}, showing a good MR signal. Concurrently, Cu^{+} and Mn^{2+} partake in a Fenton-like reaction, generating $^{\cdot}OH$ to trigger CDT. The released ICG can mediate PTT and PT imaging under laser irradiation, and upon release at the tumor site, it can enable "switched-on" FLI. In U87 tumor-bearing nude mice, intravenous injection of ICG@Mn/Cu/Zn-MOF@MnO_2 followed by laser irradiation showed rapid temperature increases at the tumor site in PT imaging results, reaching up to 56 °C within 10 minutes, sufficient to ablate the tumor. The emancipation of Mn^{2+} amplifies tumor-specific MRI signals, suggesting the drug's effective accumulation within the tumor. And the liberation of ICG post-injection manifests a pronounced findings.[117]

Apart from the combined use with fluorescent molecules, the co-application of Mn^{2+}-mediated T_1-weighted MR imaging and T_2 CAs can be used to improve the efficiency of MR imaging. Tao *et al.* incorporated Mn into the blue dye Prussian Blue (PB),

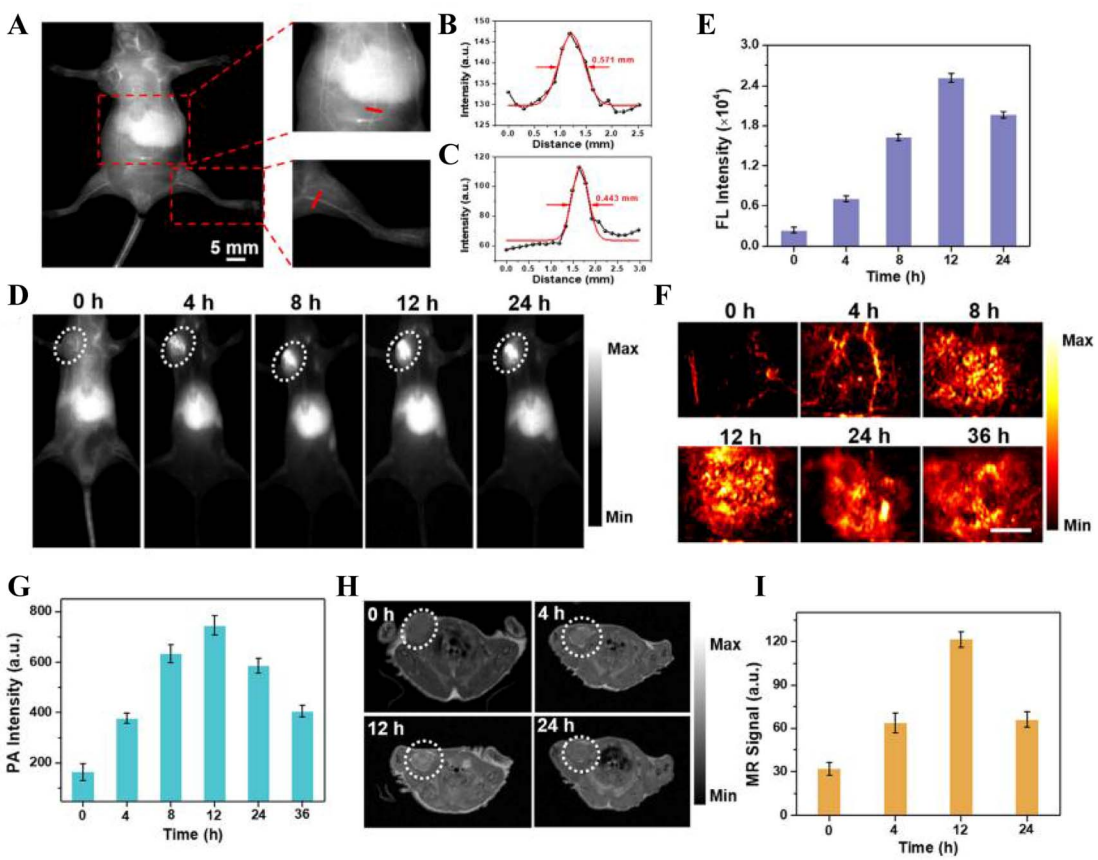

Fig. 7 *In vivo* multimodal imaging. (A) NIR-II FI of whole-body blood vessels of nude mice injected with PMR NAs solution *via* the tail vein. Fluorescence intensity profiles of the cross-sectional lines from (B) magnified abdominal vascular image and (C) magnified femoral vascular image. (D) NIR-II FI of B16F10 tumor-bearing mice injected with PMR NAs solution. (E) Mean fluorescence intensity in the tumor region. (F) PAI and (G) mean PA intensity of tumors from mice injected with PMR NAs solution. Scale bar: 3.5 mm. (H) MRI of cross-sections of mice and (I) mean MR signals of tumors after injection with PMR NAs.[116] Copyright 2023, Elsevier Ltd.

which is used for T_1 and T_2-weighted MR imaging contrast agents, to create MnPB NPs, which induce PTT when irradiated by lasers within the NIR spectrum, with their anti-tumor effects observable *via* photoacoustic imaging. Moreover, the incorporation of Mn allows MnPB NPs to engage in Fenton-like reactions, instigating CDT, while the r_1 and r_2 values of MnPB NPs were detected to be 0.6693 mM^{-1} s^{-1} and 9.379 mM^{-1} s^{-1}, both of which were significantly higher than the r_1 and r_2 values of pure PB NPs, indicating that the combination of Mn and PB could enhance MR imaging. Post intravenous injection into Skov-3 tumor-bearing mice, tri-modal *in vivo* imaging validated the formidable efficacy of MnPB NPs in tumor therapy.[118]

In summary, manganese-based nanomaterials, as ideal MRI contrast agents (CAs), have great potential in MRI-guided tumor therapy (Table 2). For augmented imaging accuracy, combining Mn-based nanomaterials with other contrast agents, facilitates the effortless attainment of multimodal imaging associated with MRI using the prepared Mn-based nanomaterials.

5 Opportunities and challenges

Overall, Mn-based CDT therapies have achieved considerable advancements. Although there have been achievements, this domain continues to encounter a myriad of opportunities and challenges. To foster the progress and clinical translation of Mn-based CDT therapy in oncology, future research should adopt a multi-faceted approach, focusing on aspects such as material fabrication, performance investigation, mechanism elucidation, and assessment of biological efficacy.

Firstly, developing simple and highly reproducible synthesis methods is crucial for promoting the biological application of Mn-based nanomaterials. The biocompatibility of Mn-based nanomaterials is indeed a crucial factor for their successful clinical translation. Recent advancements in biomimetic mineralization strategies have been particularly effective in producing Mn-based nanomaterials with enhanced biocompatibility, and it became the preferred method for preparing

Table 2 Manganese-based multi-modal imaging-guided chemodynamic therapy involving MRI

Category	Imaging modality	Contrast agents	Materials	Imaging principles	Tumor model	Administration	Ref.
Single modal imaging	Magnetic resonance imaging (MRI)	Mn^{2+}	MS@MnO_2NPs	Mn^{2+} exhibits a higher longitudinal (T_1) relaxation rate	U87MG tumor xenograft	Intratumoral injection	111
		Mn^{2+}	DOX@Mn-Alg	Providing enhanced T_1-weighted MRI contrast for diagnosis	CT26 tumor xenograft	Intravenous injection	112
		Mn^{2+}	Mn-Ti_3C_2@PEG	The magnetic properties of the Mn component allow it to serve as a T_1-weighted contrast agent for MRI	4T1 tumor xenograft	Intravenous injection	113
Dual-modal imaging	MRI and fluorescence imaging (FI)	ICG/Mn^{2+}	ICG-COP@MOF-PR	ICG conducts FI through its intrinsic fluorescence, while manganese holds the potential for MRI and possesses dual-modal imaging capabilities	OCM1 tumor xenograft	Intravenous injection	55
	MRI and photothermal (PT)	Fe^{3+}/Mn^{2+}	MnFe-LDH/MTX@GOx@Ta (MMGT)	Mn^{2+} can enhance T_1-MRI contrast signals, while MnFe-LDH can convert NIR light energy into heat for PTI	4T1 tumor xenograft	Intravenous injection	114
	MRI and computed tomography (CT) scan	Au NPs/Mn^{2+}	DOX@Au@MMSN-Ald	Gold nanoparticles and manganese ions within the shell can provide dual-modal imaging in both CT and MRI	Orthotopic 143B tumor	Intratumoral injection	115
Multimodal imaging	MRI, fluorescence imaging and photoacoustic imaging	Mn^{2+}/NIR-II semiconductor polymer	The self-assembly of ultrasmall NIR-II semiconducting polymer dots and the toll-like receptor agonist resiquimod (R848) utilizing Mn^{2+} as coordination nodes (PMR NAs)	Ultra-small NIR-II semiconductor polymers for PAI, which also exhibit intrinsic fluorescence for FI. The released Mn^{2+} can be used for MRI	B16F10 bilateral xenograft tumor	Intravenous injection	116
	MRI, fluorescence imaging and photothermal	ICG/Mn^{2+}	ICG@Mn/Cu/Zn-MOF@MnO_2	Released Mn^{2+} can be used for MRI. ICG can mediate both PAI and FI under laser irradiation	U87 tumor xenograft	Intravenous injection	117
Other imaging	(T1/T2) MRI and photoacoustic imaging	PB/Mn^{2+}	MnPB NPs	PB and Mn^{2+} serve as contrast agents, facilitating the combined use of T_1-weighted MR imaging and T_2 contrast agents to enhance MR imaging efficiency	Skov-3 tumor xenograft	Intravenous injection	118

Mn-based nanomaterials.[119] Moreover, the surface properties of nanomaterials have a significant impact on their behavior within biological systems. Therefore, by finely modifying the surface properties of Mn-based nanomaterials, their targeting to lesion sites can be significantly enhanced, improving their drug delivery efficiency. This not only enhances the therapeutic effect of CDT but also helps to improve the efficacy of other treatments like chemotherapy and reduces side effects, making the treatment process safer and more effective. In general, the research and application horizons of Mn-based CDT therapy are extensive. However, systematic and comprehensive research is still necessary to further elevate its therapeutic efficiency and clinical viability, thereby optimally serving tumor therapy.

Secondly, further research into the ROS generation mechanism underpinning CDT of Mn-based nanomaterials is crucial for steering the development of multifunctional manganese-based nano-platforms. While ROS generation *via* Fenton/Fenton-like reactions has been thoroughly investigated, however, the principles of classical catalytic chemistry may not adequately apply to intricate physiological contexts. An enhanced comprehension of the CDT process within living organisms could improve the efficacy of CDT and address challenges such as the scarcity of H_2O_2 and low pH levels in the TME. Besides thoroughly researching mechanisms related to tumor therapy based on the Fenton reaction, it's also essential to delve into ROS generation mechanisms based on non-Fenton reactions. It's critical for the development of effective Mn-based nanotherapeutic platforms to extensively study various CDT mechanisms and their synergistic interactions with other treatment modalities.[120] This involves not just studying their behavior in various tumor microenvironments, but also how to enhance therapeutic outcomes by manipulating the TME or other biological processes, and how to integrate them with other treatment strategies (such as chemotherapy, radiotherapy, *etc.*) to achieve a comprehensive attack on tumors. A comprehensive grasp and application-oriented research into the anti-tumor mechanisms of Mn-based nanomaterials not only aids in devising more efficacious tumor treatment strategies but also establishes a robust foundation for the clinical transition and application of Mn-based nanomaterials.

Finally, comprehensive investigation into the biocompatibility and biosafety of Mn-based nano-platforms is vital for their clinical conversion. This primarily includes, but is not limited to, research on cytotoxicity, hemocompatibility, tissue compatibility, immunogenicity, and pharmacokinetics. A comprehensive assessment of Mn-based nano-platforms remains indispensable before advancing to clinical applications. Although preliminary results indicate that Mn-based nanomaterials exhibit good biocompatibility during treatment, the strong oxidative effect of manganese ions poses serious side effects to the liver and kidneys.[46] Moreover, the low bioavailability and low degradation rate of free manganese ions present long-term toxicity issues to the human body. Therefore, developing ultra-small or biodegradable Mn-based nanomaterials is a favorable approach to achieving rapid metabolism and elimination from the body, thereby enhancing biosafety.[121] Simultaneously, enhancing the targeted delivery of Mn-based nanomaterials can maximize the bioavailability of nanomedicine at specific sites and times. Such targeted nanomedicines not only help reduce the dosage but also minimize the side effects of the drugs, thereby increasing biosafety.[122] Currently, the biosafety assessment of Mn-based nanomaterials largely relies on *in vitro* cell viability tests,[123] and in order to accelerate the translation to clinical applications, future studies should not be limited to small animal models (*e.g.*, mice, rats), but also large animal models (*e.g.*, monkeys) can be constructed to comprehensively assess the biosafety and efficacy of Mn-based nanoplatforms. Such research can not only provide more in-depth biosafety data but also reveal potential biological effects and mechanisms, offering a more solid scientific foundation for clinical applications. Additionally, the MRI imaging-guided feature of Mn-based nanomaterials is critically important for monitoring drug metabolic pathways and tissue distribution throughout the treatment process. These studies will assist in understanding the behavior of drugs in the body, how they interact with biological systems, and how to optimize dosing and administration strategies, to maximize therapeutic effects, minimize side effects, and provide important insights for their clinical translation. In summary, based on their biosafety and biological performance assessment, Mn-based CDT therapies are highly likely to pave a promising path in the field of nanomedicine, offering new strategies for tumor therapy.

6 Conclusions

Manganese is a trace element crucial for human health, participating in and playing a significant role in various physiological processes. Particularly in the field of nanomedicine, manganese exhibits unique functions, such as applications in immune defense, chemodynamic therapy (CDT), magnetic resonance imaging (MRI), and tumor microenvironment (TME) modulation. Among these applications, the CDT and immune defense capabilities contribute to the combined application of CDT and im-munotherapy, while TME modulation can enhance the effects of tumor therapy. The MRI capability is utilized to monitor the progression of tumor therapy. Hence, Mn-based nano-platforms emerge as optimal choices for tumor therapy tracking. In tumor CDT, Mn-based nanomaterials are extensively used not only as nanocarriers for drug delivery to tumor sites, but manganese ions also serve as important components within the nanomaterials, participating in tumor therapy. However, due to the heterogeneity and complexity of tumors, the effectiveness of single Mn-based CDT may be limited. Recognizing this challenge, recent years have seen the development of multimodal synergistic therapy strategies aimed at enhancing therapeutic outcomes while reducing drug side effects, involving the use of manganese-based nanomaterials combined with a variety of therapeutic drugs. Manganese-based nanomaterials indeed show significant promise in the creation of multifunctional nanoprobe systems, which combine MRI with other imaging methods and can be used to monitor the tumor treatment

process and evaluate therapeutic effects. There is still a long way to go for the development of Mn-based nanomaterials, and constantly exploring their applications with new perspectives, we believe that they will be of great significance for the treatment of cancer in the future.

Author contributions

M. W. was involved in literature review, writing the original draft and editing. Y. L. was involved in figure creation and editing. D. G. was involved in table creation and editing. M. Z. was involved in visualization. D. X. was involved in software. Z. Z. was involved in writing and editing. X. L. was involved in writing and methodology. Y. H. was involved in writing, editing, supervision and funding acquisition. All authors have read and agreed to the published version of the manuscript.

Conflicts of interest

There are no conflicts to declare.

Acknowledgements

We gratefully acknowledge support from the Guangxi Science and Technology Major Program (No. AA24011005), the National Nature Science Foundation of China (No. 82072340), and the Scientific and Technological Innovation Major Base of Guangxi (No. 2022-36-Z05).

Notes and references

1 R. L. Siegel, K. D. Miller, N. S. Wagle and A. Jemal, *Ca-Cancer J. Clin.*, 2023, **73**, 17–48.
2 H. Sung, J. Ferlay, R. L. Siegel, M. Laversanne, I. Soerjomataram, A. Jemal and F. Bray, *Ca-Cancer J. Clin.*, 2021, **71**, 209–249.
3 Q. Dong, T. Xue, H. Yan, F. Liu, R. Liu, K. Zhang, Y. Chong, J. Du and H. Zhang, *J. Nanobiotechnol.*, 2023, **21**, 395.
4 B. Farhood, K. Mortezaee, E. Motevaseli, H. Mirtavoos-Mahyari, D. Shabeeb, A. Eleojo Musa, N. S. Sanikhani, M. Najafi and A. Ahmadi, *J. Cell. Biochem.*, 2019, **120**, 18559–18571.
5 Q. Wang, Y. Ji, J. Shi and L. Wang, *ACS Appl. Mater. Interfaces*, 2020, **12**, 23677–23688.
6 Z. Tang, Y. Liu, M. He and W. Bu, *Angew Chem. Int. Ed. Engl.*, 2019, **58**, 946–956.
7 P. Yang, J. Tao, F. Chen, Y. Chen, J. He, K. Shen, P. Zhao and Y. Li, *Small*, 2021, **17**, e2005865.
8 X. J. Yang, X. M. Xu, J. Xu and Y. F. Han, *J. Am. Chem. Soc.*, 2013, **135**, 16058–16061.
9 H. Li, R. Cheng, Z. Liu and C. Du, *Sci. Total Environ.*, 2019, **683**, 638–647.
10 Z. Yu, Y. Hu, Y. Sun and T. Sun, *Chemistry*, 2021, **27**, 13953–13960.
11 H. Mei, J. Han, S. White, D. J. Graham, K. Izawa, T. Sato, S. Fustero, N. A. Meanwell and V. A. Soloshonok, *Chemistry*, 2020, **26**, 11349–11390.
12 C. Qiao, R. Zhang, Y. Wang, Q. Jia, X. Wang, Z. Yang, T. Xue, R. Ji, X. Cui and Z. Wang, *Angew Chem. Int. Ed. Engl.*, 2020, **59**, 16982–16988.
13 L. Zhou, J. Chen, Y. Sun, K. Chai, Z. Zhu, C. Wang, M. Chen, W. Han, X. Hu, R. Li, T. Yao, H. Li, C. Dong and S. Shi, *J. Nanobiotechnol.*, 2021, **19**, 261.
14 P. Zhao, H. Li and W. Bu, *Angew Chem. Int. Ed. Engl.*, 2023, **62**, e202210415.
15 W. N. Zhao, H. Li, S. Sun and Y. Xu, *J. Mater. Chem. B*, 2023, **11**, 11044–11051.
16 J. Tan, X. Duan, F. Zhang, X. Ban, J. Mao, M. Cao, S. Han, X. Shuai and J. Shen, *Adv. Sci.*, 2020, **7**, 2003036.
17 G. K. Kirschner, *Plant J.*, 2023, **116**, 1551–1552.
18 J. M. Studer, W. P. Schweer, N. K. Gabler and J. W. Ross, *Anim. Reprod. Sci.*, 2022, **238**, 106924.
19 A. C. Martins, B. N. Krum, L. Queirós, A. A. Tinkov, A. V. Skalny, A. B. Bowman and M. Aschner, *J. Agric. Food Chem.*, 2020, **68**, 12893–12903.
20 D. M. Wang, R. R. Zhu, Y. Tian, K. Uludag, J. J. Chen, H. X. Zhou, L. Wang, T. R. Kosten and X. Y. Zhang, *Antioxidants*, 2022, **11**(10), 1981.
21 P. Chen, J. Bornhorst and M. Aschner, *Front. Biosci.*, 2018, **23**, 1655–1679.
22 Q. Wu, Q. Mu, Z. Xia, J. Min and F. Wang, *Semin. Cell Dev. Biol.*, 2021, **115**, 45–53.
23 D. Budinger, S. Barral, A. K. S. Soo and M. A. Kurian, *Lancet Neurol.*, 2021, **20**, 956–968.
24 J. Fernandes, J. D. Chandler, K. H. Liu, K. Uppal, L. Hao, X. Hu, Y. M. Go and D. P. Jones, *Toxicol. Sci.*, 2019, **169**, 84–94.
25 M. Lv, M. Chen, R. Zhang, W. Zhang, C. Wang, Y. Zhang, X. Wei, Y. Guan, J. Liu, K. Feng, M. Jing, X. Wang, Y. C. Liu, Q. Mei, W. Han and Z. Jiang, *Cell Res.*, 2020, **30**, 966–979.
26 C. Jia, Y. Guo and F. G. Wu, *Small*, 2022, **18**, e2103868.
27 H. H. Fan and Z. J. Guo, *Coord. Chem. Rev.*, 2023, **480**, 215027.
28 B. M. Sahoo, B. K. Banik, P. Borah and A. Jain, *Adv. Anticancer Agents Med. Chem.*, 2022, **22**, 215–222.
29 M. Y. Chen, C. Y. Dong and S. Shi, *ACS Mater. Lett.*, 2022, **4**, 2415–2433.
30 K. Wang, Y. Dong, J. Liu, L. Qian, T. Wang, X. Gao, K. Wang and L. Zhou, *Oxid. Med. Cell. Longevity*, 2020, **2020**, 5860356.
31 W. Yu, F. Jia, J. Fu, Y. Chen, Y. Huang, Q. Jin, Y. Wang and J. Ji, *ACS Nano*, 2023, **17**, 15713–15723.
32 Z. H. Zhou, S. Y. Liang, T. C. Zhao, X. Z. Chen, X. K. Cao, M. Qi, Y. Y. Huang, W. T. Ju, M. Yang, D. W. Zhu, Y. C. Pang and L. P. Zhong, *J. Nanobiotechnol.*, 2021, **19**, 157.
33 R. Liang, L. Liu, H. He, Z. Chen, Z. Han, Z. Luo, Z. Wu, M. Zheng, Y. Ma and L. Cai, *Biomaterials*, 2018, **177**, 149–160.
34 X. Liu, Y. Jin, T. Liu, S. Yang, M. Zhou, W. Wang and H. Yu, *ACS Biomater. Sci. Eng.*, 2020, **6**, 4834–4845.
35 X. Zhong, X. Dai, Y. Wang, H. Wang, H. Qian and X. Wang, *Wiley Interdiscip. Rev.: Nanomed. Nanobiotechnol.*, 2022, **14**, e1797.

36 J. Y. Lu, Y. Q. Yang, Q. Q. Xu, Y. Z. Lin, S. P. Feng, Y. L. Mao, D. Wang, S. L. Wang and Q. F. Zhao, *Coord. Chem. Rev.*, 2023, **474**, 214861.
37 Z. Zhao, Z. Ma, B. Wang, Y. Guan, X. D. Su and Z. Jiang, *Cell Rep.*, 2020, **32**, 108053.
38 P. Song, W. Yang, K. F. Lou, H. Dong, H. Zhang, B. Wang and D. Chen, *EMBO Rep.*, 2022, **23**, e55099.
39 X. Y. Ma, M. M. Chen and L. H. Meng, *Acta Pharmacol. Sin.*, 2023, 1–10.
40 X. Wang, M. Lin, L. Zhu and Z. Ye, *Front. Immunol.*, 2023, **14**, 1200245.
41 Z. Sun and V. Hornung, *Curr. Biol.*, 2022, **32**, R730–r734.
42 C. Wang, Y. Guan, M. Lv, R. Zhang, Z. Guo, X. Wei, X. Du, J. Yang, T. Li, Y. Wan, X. Su, X. Huang and Z. Jiang, *Immunity*, 2018, **48**, 675–687.
43 G. Reale, F. Calderoni, T. Ghirardi, F. Porto, F. Illuminati, L. Marvelli, P. Martini, L. Uccelli, E. Tonini, L. Del Bianco, F. Spizzo, M. Capozza, E. Cazzola, A. Carnevale, M. Giganti, A. Turra, J. Esposito and A. Boschi, *Int. J. Mol. Sci.*, 2023, **24**(4), 3461.
44 R. Antwi-Baah, Y. J. Wang, X. Q. Chen and K. Yu, *Adv. Mater. Interfaces*, 2022, **9**(9), 2101710.
45 S. Daksh, A. Kaul, S. Deep and A. Datta, *J. Inorg. Biochem.*, 2022, **237**, 112018.
46 O. U. Akakuru, M. Z. Iqbal, M. Saeed, C. Liu, T. Paunesku, G. Woloschak, N. S. Hosmane and A. Wu, *Bioconjugate Chem.*, 2019, **30**, 2264–2286.
47 B. T. Bedenk, S. Almeida-Corrêa, A. Jurik, N. Dedic, B. Grünecker, A. J. Genewsky, S. F. Kaltwasser, C. J. Riebe, J. M. Deussing, M. Czisch and C. T. Wotjak, *Neuroimage*, 2018, **169**, 374–382.
48 P. F. Yang, D. Y. Chen, J. W. Hu, J. H. Chen and C. T. Yen, *Pain*, 2011, **152**, 194–203.
49 P. Mi, D. Kokuryo, H. Cabral, H. Wu, Y. Terada, T. Saga, I. Aoki, N. Nishiyama and K. Kataoka, *Nat. Nanotechnol.*, 2016, **11**, 724–730.
50 L. Yang, L. Wang, G. Huang, X. Zhang, L. Chen, A. Li, J. Gao, Z. Zhou, L. Su, H. Yang and J. Song, *Theranostics*, 2021, **11**, 6966–6982.
51 C. Li, M. Wang, P. F. Li, J. Sheng and Q. Fu, *Small*, 2024, e2306257, DOI: **10.1002/smll.202306257**.
52 H. Sabit, M. Abdel-Hakeem, T. Shoala, S. Abdel-Ghany, M. M. Abdel-Latif, J. Almulhim and M. Mansy, *Pharmaceutics*, 2022, **14**(8), 1566.
53 K. K. Jain, *Trends Biotechnol.*, 2006, **24**, 143–145.
54 X. Chen, D. Cheng, N. Yu, J. Feng, J. Li and L. Lin, *J. Mater. Chem. B*, 2024, **12**, 1296–1306.
55 Y. Li, F. Li, H. Pan, X. Huang, J. Yu, X. Liu, Q. Zhang, C. Xiao, H. Zhang and L. Zhang, *J. Nanobiotechnol.*, 2022, **20**, 472.
56 X. Zhong, X. Bao, H. Zhong, Y. Zhou, Z. Zhang, Y. Lu, Q. Dai, Q. Yang, P. Ke, Y. Xia, L. Wu, Z. Sui, Y. Lu, M. Han, W. Xu and J. Gao, *Int. J. Pharm.*, 2022, **622**, 121810.
57 Brianna and S. H. Lee, *Med. Oncol.*, 2023, **40**, 88.
58 Y. Hussain, L. Islam, H. Khan, R. Filosa, M. Aschner and S. Javed, *Phytother. Res.*, 2021, **35**, 6514–6529.
59 P. Jain, A. K. Jangid, D. Pooja and H. Kulhari, *J. Mater. Chem. B*, 2024, **12**, 577–608.
60 D. Pe'er, S. Ogawa, O. Elhanani, L. Keren, T. G. Oliver and D. Wedge, *Cancer Cell*, 2021, **39**, 1015–1017.
61 G. Marwaha, R. Macklis, A. D. Singh and A. Wilkinson, *Dev. Ophthalmol.*, 2013, **52**, 29–35.
62 S. Keam, S. Gill, M. A. Ebert, A. K. Nowak and A. M. Cook, *Clin. Transl. Immunol.*, 2020, **9**(9), e1169.
63 S. Pan, Z. Sun, B. Zhao, L. Miao, Q. Zhou, T. Chen and X. Zhu, *Biomaterials*, 2023, **302**, 122321.
64 X. D. Wang, C. Y. Wang, H. M. Tian, B. L. Wu and W. Cheng, *Adv. Ther.*, 2023, 2300265.
65 J. Li, Z. You, S. Zhai, J. Zhao and K. Lu, *ACS Appl. Mater. Interfaces*, 2023, **15**, 21941–21952.
66 H. Chen, D. Zhu, L. Guo and G. Li, *Int. J. Nanomedicine*, 2022, **17**, 1005–1014.
67 X. H. Lin, R. Zhu, Z. Z. Hong, X. Zhang, S. Chen, J. B. Song and H. H. Yang, *Adv. Funct. Mater.*, 2021, **31**(24), 2101278.
68 X. Y. Liu, Y. X. Zhu, H. R. Jia, X. P. Zhang, G. Gao, K. F. Xu, X. W. Yu, S. H. Wang, Z. X. Wang, P. H. Zhen, G. L. Liang and F. G. Wu, *Mater. Today Nano*, 2023, **24**(2), 168–170.
69 W. Cao, M. Jin, K. Yang, B. Chen, M. Xiong, X. Li and G. Cao, *J. Nanobiotechnol.*, 2021, **19**, 325.
70 J. Xiao, G. Zhang, R. Xu, H. Chen, H. Wang, G. Tian, B. Wang, C. Yang, G. Bai, Z. Zhang, H. Yang, K. Zhong, D. Zou and Z. Wu, *Biomaterials*, 2019, **216**, 119254.
71 L. Chen, S. F. Zhou, L. Su and J. Song, *ACS Nano*, 2019, **13**, 10887–10917.
72 D. Jin, J. Zhang, Y. Huang, X. Qin, J. Zhuang, W. Yin, S. Chen, Y. Wang, P. Hua and Y. Yao, *Dalton Trans.*, 2021, **50**, 1189–1196.
73 Y. Zhou, T. Yang, K. Liang and R. Chandrawati, *Adv. Drug Delivery Rev.*, 2021, **171**, 199–214.
74 T. He, X. Qin, C. Jiang, D. Jiang, S. Lei, J. Lin, W. G. Zhu, J. Qu and P. Huang, *Theranostics*, 2020, **10**, 2453–2462.
75 B. Zhao, P. Zhao, Z. Jin, M. Fan, J. Meng and Q. He, *J. Nanobiotechnol.*, 2019, **17**, 75.
76 J. H. Correia, J. A. Rodrigues, S. Pimenta, T. Dong and Z. Yang, *Pharmaceutics*, 2021, **13**(9), 1332.
77 L. Larue, B. Myrzakhmetov, A. Ben-Mihoub, A. Moussaron, N. Thomas, P. Arnoux, F. Baros, R. Vanderesse, S. Acherar and C. Frochot, *Pharmaceuticals*, 2019, **12**(4), 163.
78 H. Hou, X. Huang, G. Wei, F. Xu, Y. Wang and S. Zhou, *ACS Appl. Mater. Interfaces*, 2019, **11**, 29579–29592.
79 W. Sun, T. Shi, L. Luo, X. Chen, P. Lv, Y. Lv, Y. Zhuang, J. Zhu, G. Liu, X. Chen and H. Chen, *Adv. Mater.*, 2019, **31**, e1808024.
80 Q. Li, W. Li, H. Di, L. Luo, C. Zhu, J. Yang, X. Yin, H. Yin, J. Gao, Y. Du and J. You, *J. Controlled Release*, 2018, **277**, 114–125.
81 P. Wang, C. Liang, J. Zhu, N. Yang, A. Jiao, W. Wang, X. Song and X. Dong, *ACS Appl. Mater. Interfaces*, 2019, **11**, 41140–41147.
82 C. Liu, D. Wang, S. Zhang, Y. Cheng, F. Yang, Y. Xing, T. Xu, H. Dong and X. Zhang, *ACS Nano*, 2019, **13**, 4267–4277.
83 J. Roy, V. Pandey, I. Gupta and H. Shekhar, *ACS Biomater. Sci. Eng.*, 2021, **7**, 5326–5338.

84 Q. L. Guo, X. L. Dai, M. Y. Yin, H. W. Cheng, H. S. Qian, H. Wang, D. M. Zhu and X. W. Wang, *Mil. Med. Res.*, 2022, **9**, 26.
85 H. Lin, Y. Chen and J. Shi, *Chem. Soc. Rev.*, 2018, **47**, 1938–1958.
86 J. Xin, C. Deng, O. Aras, M. Zhou, C. Wu and F. An, *J. Nanobiotechnol.*, 2021, **19**, 192.
87 F. Jiang, C. Z. Yang, B. B. Ding, S. Liang, Y. J. Zhao, Z. Y. Cheng, M. Liu, B. G. Xing, P. A. Ma and J. Lin, *Chin. Chem. Lett.*, 2022, **33**, 2959–2964.
88 L. Sun, Y. Cao, W. Li, L. Wang, P. Ding, Z. Lu, F. Ma, Z. Wang and R. Pei, *Small*, 2023, **19**, e2300101.
89 P. Xu and F. Liang, *Int. J. Nanomedicine*, 2020, **15**, 9159–9180.
90 Z. Chen, Z. Li, C. Li, H. Huang, Y. Ren, Z. Li, Y. Hu and W. Guo, *Drug Delivery*, 2022, **29**, 1201–1211.
91 S. R. Dash and C. N. Kundu, *Curr. Nanosci.*, 2022, **18**, 31–47.
92 A. C. V. Doughty, A. R. Hoover, E. Layton, C. K. Murray, E. W. Howard and W. R. Chen, *Materials*, 2019, **12**(5), 779.
93 C. Li, Y. Cheng, D. Li, Q. An, W. Zhang, Y. Zhang and Y. Fu, *Int. J. Mol. Sci.*, 2022, **23**(14), 7909.
94 X. Ma, B. Chen, H. Wu, Q. Jin, W. Wang, Z. Zha, H. Qian and Y. Ma, *J. Mater. Chem. B*, 2022, **10**, 3452–3461.
95 Y. Guo, F. Gao, A. Ahmed, M. Rafiq, B. Yu, H. Cong and Y. Shen, *J. Mater. Chem. B*, 2023, **11**, 8586–8604.
96 W. Jiang, Y. Wang, J. A. Wargo, F. F. Lang and B. Y. S. Kim, *Nat. Nanotechnol.*, 2021, **16**, 6–15.
97 R. Zhang, C. Wang, Y. Guan, X. Wei, M. Sha, M. Yi, M. Jing, M. Lv, W. Guo, J. Xu, Y. Wan, X. M. Jia and Z. Jiang, *Cell. Mol. Immunol.*, 2021, **18**, 1222–1234.
98 Y. Shi and T. Lammers, *Acc. Chem. Res.*, 2019, **52**, 1543–1554.
99 J. Chen, J. X. Lu, Y. Y. Shan, Y. Q. Wang, Z. L. Xu, J. Q. Xi, L. Fan and L. Z. Gao, *Adv. Ther.*, 2023, **6**(3), 2200175.
100 X. Deng, T. Liu, Y. Zhu, J. Chen, Z. Song, Z. Shi and H. Chen, *Bioact. Mater.*, 2024, **33**, 483–496.
101 R. Wu, Q. Min, J. Guo, T. Zheng, L. Jiang and J. J. Zhu, *Anal. Chem.*, 2019, **91**, 4608–4617.
102 J. Wang, W. Kong, H. Jin, C. Li, Q. Luo, Y. Luo, C. Yuan, J. Lu, L. Zhang and X. Liu, *Colloids Surf., B*, 2022, **218**, 112750.
103 A. Dong, S. Huang, Z. Qian, S. Xu, W. Yuan and B. Wang, *J. Mater. Chem. B*, 2023, **11**, 10883–10895.
104 L. H. Fu, Y. R. Hu, C. Qi, T. He, S. Jiang, C. Jiang, J. He, J. Qu, J. Lin and P. Huang, *ACS Nano*, 2019, **13**, 13985–13994.
105 D. Gu, Z. Liu, H. Wu, P. An, X. Zhi, Y. Yin, W. Liu and B. Sun, *Colloids Surf., B*, 2021, **199**, 111538.
106 L. Dai, M. Yao, Z. Fu, X. Li, X. Zheng, S. Meng, Z. Yuan, K. Cai, H. Yang and Y. Zhao, *Nat. Commun.*, 2022, **13**, 2688.
107 S. Guan, X. Liu, C. Li, X. Wang, D. Cao, J. Wang, L. Lin, J. Lu, G. Deng and J. Hu, *Small*, 2022, **18**, e2107160.
108 Y. Wang, D. Jing, J. Yang, S. Zhu, J. Shi, X. Qin, W. Yin, J. Wang, Y. Ding, T. Chen, B. Lu and Y. Yao, *Acta Biomater.*, 2022, **154**, 467–477.
109 M. Chang, M. Wang, M. Wang, M. Shu, B. Ding, C. Li, M. Pang, S. Cui, Z. Hou and J. Lin, *Adv. Mater.*, 2019, **31**, e1905271.
110 K. I. Matsumoto, J. B. Mitchell and M. C. Krishna, *Molecules*, 2021, **26**(6), 1614.
111 L. S. Lin, J. Song, L. Song, K. Ke, Y. Liu, Z. Zhou, Z. Shen, J. Li, Z. Yang, W. Tang, G. Niu, H. H. Yang and X. Chen, *Angew Chem. Int. Ed. Engl.*, 2018, **57**, 4902–4906.
112 M. Su, Y. Q. Zhu, J. B. Chen, B. B. Zhang, C. Y. Sun, M. W. Chen and X. Z. Yang, *Chem. Eng. J.*, 2022, **435**, 134926.
113 D. An, X. Wu, Y. L. Gong, W. L. Li, G. D. Dai, X. F. Lu, L. M. Yu, W. X. Ren, M. Qiu and J. Shu, *Nanophotonics*, 2022, **11**, 5177–5188.
114 B. Zhu, M. Zhang, Q. Chen, Z. Li, S. Chen and J. Zhu, *Biomater. Sci.*, 2023, **11**, 2129–2138.
115 Z. Sha, S. Yang, L. Fu, M. Geng, J. Gu, X. Liu, S. Li, X. Zhou and C. He, *Nanoscale*, 2021, **13**, 5077–5093.
116 Y. Dai, X. Li, Y. Xue, K. Chen, G. Jiao, L. Zhu, M. Li, Q. Fan, Y. Dai, Q. Zhao and Q. Shen, *Acta Biomater.*, 2023, **166**, 496–511.
117 Y. Cheng, C. Wen, Y. Q. Sun, H. Yu and X. B. Yin, *Adv. Funct. Mater.*, 2021, **31**(37), 2104378.
118 Q. Tao, G. He, S. Ye, D. Zhang, Z. Zhang, L. Qi and R. Liu, *J. Nanobiotechnol.*, 2022, **20**, 18.
119 C. Qi, J. He, L. H. Fu, T. He, N. T. Blum, X. Yao, J. Lin and P. Huang, *ACS Nano*, 2021, **15**, 1627–1639.
120 X. W. Wang, X. Y. Zhong, Z. Liu and L. Cheng, *Nano Today*, 2020, **35**, 100946.
121 Z. Miao, S. Chen, C. Y. Xu, Y. Ma, H. Qian, Y. Xu, H. Chen, X. Wang, G. He, Y. Lu, Q. Zhao and Z. Zha, *Chem. Sci.*, 2019, **10**, 5435–5443.
122 H. Su, Y. Wang, Y. Gu, L. Bowman, J. Zhao and M. Ding, *J. Appl. Toxicol.*, 2018, **38**, 3–24.
123 J. Fei, Y. Liu, Y. Zeng, M. Yang, S. Chen, X. Duan, L. Lu and M. Chen, *Front. Bioeng. Biotechnol.*, 2024, **12**, 1363569.